



Synthesis paper

The role of changing geodynamics in the progressive contamination of Late Cretaceous to Late Miocene arc magmas in the southern Central Andes



Rosemary E. Jones^{a,b,*}, Linda A. Kirstein^a, Simone A. Kasemann^c, Vanesa D. Litvak^d, Stella Poma^e, Ricardo N. Alonso^f, Richard Hinton^a, EIMF^g

^a School of GeoSciences, University of Edinburgh, The King's Buildings, James Hutton Road, Edinburgh EH9 3FE, UK

^b Department of Earth Sciences, University of Oxford, South Parks Road, Oxford OX1 3AN, UK

^c Faculty of Geosciences & MARUM, Centre for Marine Environmental Sciences, University of Bremen, 28334 Bremen, Germany

^d Universidad de Buenos Aires, CONICET, Instituto de Estudios Andinos Don Pablo Groeber (IDEAN), Facultad de Ciencias Exactas y Naturales, Buenos Aires, Argentina

^e Universidad de Buenos Aires, CONICET, Instituto de Geociencias Básicas y Aplicadas de Buenos Aires (IGABA), Facultad de Ciencias Exactas y Naturales, Buenos Aires, Argentina

^f Departamento de Geología, Universidad Nacional de Salta, CONICET, 4400 Salta, Argentina

^g Edinburgh Ion Microprobe Facility, School of GeoSciences, University of Edinburgh, West Mains Road, Edinburgh EH9 3JW, UK

ARTICLE INFO

Article history:

Received 4 April 2016

Accepted 1 July 2016

Available online 14 July 2016

Keywords:

Central Andes

Geochronology

Arc magma petrogenesis

Crustal contamination

Geodynamics

ABSTRACT

The tectonic and geodynamic setting of the southern Central Andean convergent margin changed significantly between the Late Cretaceous and the Late Miocene, influencing magmatic activity and its geochemical composition. Here we investigate how these changes, which include changing slab-dip angle and convergence angles and rates, have influenced the contamination of the arc magmas with crustal material. Whole rock geochemical data for a suite of Late Cretaceous to Late Miocene arc rocks from the Pampean flat-slab segment (29–31 °S) of the southern Central Andes is presented alongside petrographic observations and high resolution age dating. In-situ U–Pb dating of magmatic zircon, combined with Ar–Ar dating of plagioclase, has led to an improved regional stratigraphy and provides an accurate temporal constraint for the geochemical data.

A generally higher content of incompatible trace elements (e.g. Nb/Zr ratios from 0.019 to 0.083 and Nb/Yb from 1.5 to 16.4) is observed between the Late Cretaceous (~72 Ma), when the southern Central Andean margin is suggested to have been in extension, and the Miocene when the thickness of the continental crust increased and the angle of the subducting Nazca plate shallowed. Trace and rare earth element compositions obtained for the Late Cretaceous to Late Eocene arc magmatic rocks from the Principal Cordillera of Chile, combined with a lack of zircon inheritance, suggest limited assimilation of the overlying continental crust by arc magmas derived from the mantle wedge. A general increase in incompatible, fluid-mobile/immobile (e.g., Ba/Nb) and fluid-immobile/immobile (e.g., Nb/Zr) trace element ratios is attributed to the influence of the subducting slab on the melt source region and/or the influx of asthenospheric mantle.

The Late Oligocene (~26 Ma) to Early Miocene (~17 Ma), and Late Miocene (~6 Ma) arc magmatic rocks present in the Frontal Cordillera show evidence for the bulk assimilation of the Permian–Triassic (P–T) basement, both on the basis of their trace and rare earth element compositions and the presence of P–T inherited zircon cores. Crustal reworking is also identified in the Argentinean Precordillera; Late Miocene (12–9 Ma) arc magmatic rocks display distinct trace element signatures (specifically low Th, U and REE concentrations) and contain inherited zircon cores with Proterozoic and P–T ages, suggesting the assimilation of both the P–T basement and a Grenville-aged basement. We conclude that changing geodynamics play an important role in determining the geochemical evolution of magmatic rocks at convergent margins and should be given due consideration when evaluating the petrogenesis of arc magmas.

© 2016 Published by Elsevier B.V.

1. Introduction

Subduction zones are the principal sites for the production of new continental crust through the production of arc magmas. Determining the relative contributions to arc magmas from the mantle, subducting

* Corresponding author at: Department of Earth Sciences, University of Oxford, South Parks Road, Oxford OX1 3AN, UK. Tel.: +44 1865 272000.

E-mail address: Rosie.Jones@earth.ox.ac.uk (R.E. Jones).

components (e.g., sediments, oceanic crust) and pre-existing crust, are key to quantifying rates of crustal growth and recycling over time. Crustal material can either be incorporated into arc magmas in the melt source region, due to the subduction of sediments/subduction erosion of overriding lithosphere, and/or due to the assimilation of the overlying crust as arc magmas migrate towards the surface. The Andean margin has been an important site for continental crust production throughout the Cenozoic and is a type locality of an ocean-continent convergent margin.

The recycling of crustal material to Andean arc magmas has been long identified, however the mode of recycling is widely debated. Although most authors agree that there is an increase in the contributions to Central Andean arc magmas from crustal derived material over the course of the Cenozoic, the origin (i.e., subducted crustal material or the overlying Andean crust) of these crustal signatures remains unresolved. The contamination of the melt source region with subducted sediments (e.g., Kilian and Behrmann, 2003; Lucassen et al., 2010; Sigmarsson et al., 1990), crustal material from subduction erosion (e.g., Goss et al., 2013; Kay et al., 2005; Stern, 1991), melts derived from the subducting oceanic plate (e.g., Reich et al., 2003; Stern and Kilian, 1996), as well as the contamination of arc magmas during ascent through the continental crust (e.g., Davidson et al., 1991; Hildreth and Moor bath, 1988; James, 1982; Wörner et al., 1992), has all previously been invoked to explain the petrological and geochemical characteristics of arc magmatic rocks from the Andean margin.

The Andean margin is segmented along its length, with different segments being influenced by different tectonic regimes and geodynamic settings (e.g., Jordan et al., 1983; Pilger, 1981). The geodynamic setting of the southern Central Andean margin has changed significantly over the course of the Cenozoic. Specifically, the angle at which the Nazca plate subducted beneath the South American continent shallowed during the Miocene (e.g., Cahill and Isacks, 1992; Yañez et al., 2001, 2002). This resulted in the margin developing from the extensional regime in existence during the Late Cretaceous (~75 Ma) to a highly compressive regime during the latter part of the Miocene (Jordan et al., 1983). Consequently the thickness of the continental crust increased from ~30 km to >50 km over the latter part of the Cenozoic (Allmendinger et al., 1990; Chulick et al., 2013; Fromm et al., 2004; McGlashan et al., 2008).

The shallowing of the subducting Nazca plate has been linked with the subduction of the Juan Fernandez Ridge (JFR), a hotspot-derived seamount chain which may have undergone significant hydration and serpentinisation (e.g., Gutscher et al., 2000b; Jones et al., 2014; Kay and Mpodozis, 2002; Kopp et al., 2004; Pilger, 1981; Yañez et al., 2001, 2002). The intersection and subduction of the JFR has also been associated with increased levels of subduction erosion of the fore-arc (e.g., Stern, 1991; Stern and Skewes, 1995; von Huene et al., 1997) and is thought to act as a barrier to sediment transport and the accumulation of sediments in the Chilean trench north of ~33°S (Völker et al., 2013; von Huene et al., 1997).

These changes in tectonic and geodynamic setting over time make the southern Central Andes an interesting location at which to investigate changes in the contamination of arc magmas with crustal derived material. Previous studies into the petrogenesis of Cenozoic arc magmas in this region have primarily utilised whole rock geochemistry (e.g., Bissig et al., 2003; Kay and Abbruzzi, 1996; Kay et al., 1991; Litvak and Poma, 2010; Litvak et al., 2007; Parada, 1990; Winocur et al., 2015) and have tended to focus on narrow geological timeframes or geographical areas. In this study a variety of geochronological and geochemical techniques have been applied to both plutonic and volcanic arc rocks, which have been emplaced and erupted over a wide time frame (~73–6 Ma) and over a wide across-arc extent, from the Principal Cordillera of Chile (~70.8°W) to the Argentinean Precordillera (~69.1°W), allowing a more complete picture to be established.

A comprehensive new major, trace and rare earth element data set is presented alongside the results of high resolution U–Pb and Ar–Ar age dating. Prior to this study the majority of the age information available

for the southern Central Andean arc stratigraphy has been derived from K–Ar dating (e.g., Limarino et al., 1999; Litvak and Page, 2002; Mpodozis and Cornejo, 1988; Nasi et al., 1990; Pineda and Calderón, 2008; Pineda and Emparan, 2006), combined with some Ar–Ar dating (Bissig et al., 2001) and limited U–Pb dating (Martin et al., 1997). Due to the variable effects of hydrothermal alteration on the arc magmatic rocks (e.g., Bissig et al., 2001; Litvak et al., 2007; Maksaeu et al., 1984) some of the K–Ar ages have been found to be unreliable (Winocur et al., 2015). On this basis, this study conducted high resolution in-situ U–Pb dating of magmatic zircon and Ar–Ar dating of plagioclase in order to improve the regional stratigraphy and to provide an accurate temporal constraint for the geochemical data. In addition, in-situ U–Pb dating has the potential to reveal inherited zircon cores and therefore can be used to identify the age of the continental crust being assimilated (e.g., Beard et al., 2005). Finally, the results obtained have been used to investigate the growth and evolution of the Andean continental crust and to refine geodynamic models of the evolution of the Pampean flat-slab segment.

2. The geological and geodynamic setting

The study area is located within the Pampean (Chilean) flat-slab segment (between 29 and 31°S) of the southern Central Andes and spans the Principal Cordillera, Frontal Cordillera and Precordillera of Chile and Argentina (Fig. 1). Subduction of oceanic crust beneath the South American continent has been active since the Jurassic and has produced a series of volcanic arcs (e.g., Charrier et al., 2007; Ramos et al., 2002; Stern, 2004). From the Cretaceous through to the Late Oligocene the southern Central Andes is considered to have been in extension (e.g., Charrier et al., 2007 and references therein). At ~25 Ma the oceanic Farallón plate divided into the Nazca and Cocos plates (Lonsdale, 2005). This caused an increase in convergence rates (from ~8 cm/yr to ~15 cm/yr) and a change from oblique (NE–SW) to orthogonal (ENE–WSW) convergence (Pardo Casas and Molnar, 1987; Somoza, 1998; Somoza and Ghidella, 2012). The westward migration of the South American plate is also thought to have been initiated after ~30 Ma (Silver et al., 1998). After this time the Andean margin became more compressional and the reconfiguration of the subducting oceanic plates has been linked to a period of major uplift, increased magmatic activity, and a broadening and eastward migration of the magmatic arc (Pilger, 1984). Increased convergence rates (~15 cm/yr) are thought to have been sustained up until ~20 Ma, followed by a gradual decline to present day values (~7 cm/yr) (Pilger, 1984; Somoza and Ghidella, 2012).

There is currently no active volcanism in the Pampean flat-slab segment due to the low angle at which the oceanic Nazca plate subducts beneath the South American continent (e.g., Cahill and Isacks, 1992). The JFR began intersecting the Andean continental margin during the early Miocene (~18 Ma at ~30°S) and is thought to have led to the shallowing of the subduction angle (Gutscher et al., 2000b; Jones et al., 2014; Kirby et al., 1996; Nur and Ben-Avraham, 1981; Pilger, 1981, 1984; Yañez et al., 2001, 2002). This shallowing led to a broadening and eastward migration of the magmatic arc, a reduction in magma volume, and the eventual cessation of arc magmatism in the late Miocene (~6 Ma) (Bissig et al., 2001; Kay et al., 1987; Litvak et al., 2007; Ramos et al., 1989).

3. Cenozoic arc magmatism and stratigraphy

In the southern Central Andes the Cenozoic plutonic and volcanic arc rocks occur as north–south trending belts which lie to the east of the Coastal Batholith, which is primarily late Paleozoic to early Cretaceous in age. The older, more continuous western belt was intruded in the Paleocene–Eocene and the younger more eastern belt is of Oligocene–Miocene age, demonstrating an eastward migration of magmatism with time (Parada et al., 2007) (Fig. 1). There is a geographical gap between the two belts which corresponds with a widespread lull in

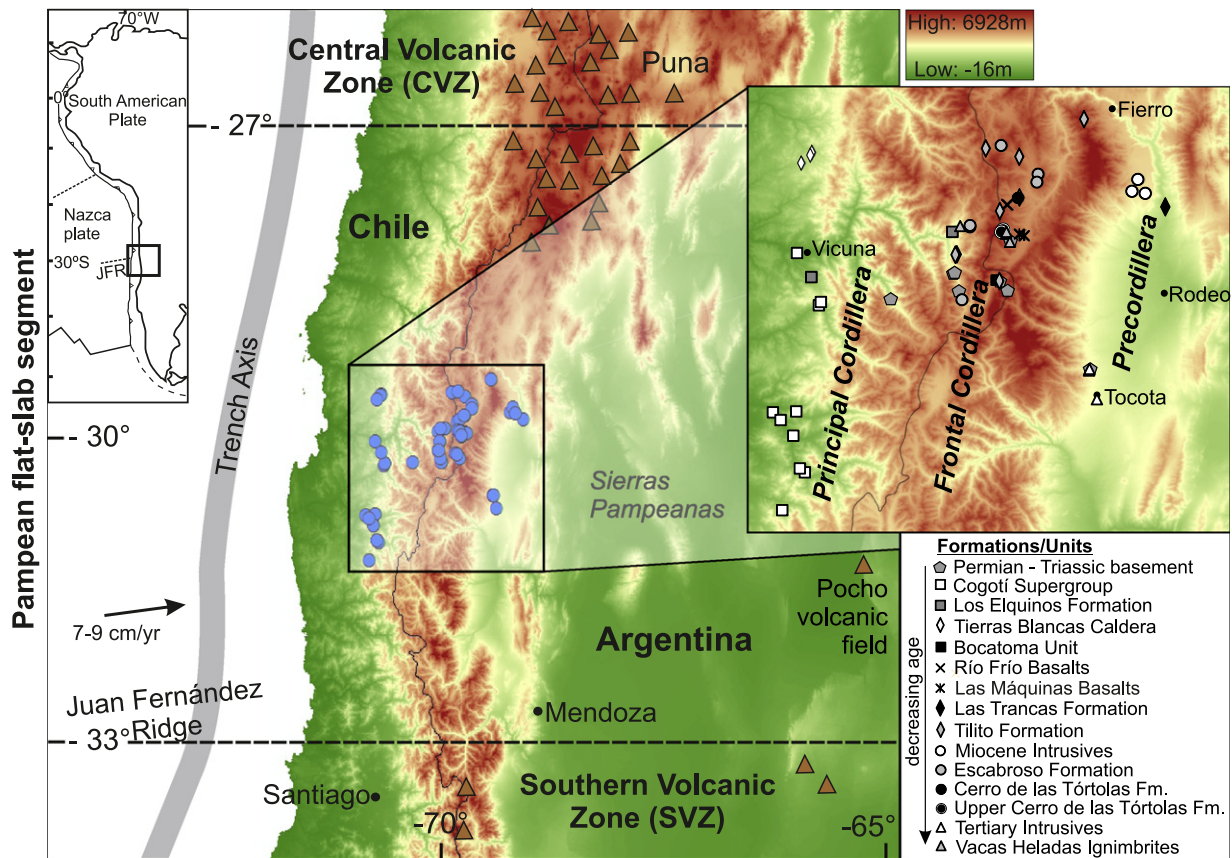


Fig. 1. Map of the study area showing the main features of the present day southern Central Andean margin. In the main map the sample locations are highlighted as blue circles and primary active volcanoes as brown triangles. In the expanded region the samples are identified by assigned geological formation/unit. Digital elevation data from Jarvis et al. (2008).

magmatic activity between ~39 and 26 Ma (Parada et al., 1988, 2007). In order to provide a context for the geochemical data, the Cenozoic arc stratigraphy for the southern Central Andes is outlined below and in Fig. 2.

The Paleocene–Eocene belt is located in the Chilean Principal Cordillera (Fig. 1) and is primarily composed of epizonal plutons which have been assembled into the Cogotí Supergroup (Parada et al., 1988). Granitoids of the Cogotí Supergroup have K–Ar ages between 67 ± 2 Ma and 38 ± 1 Ma (Parada et al., 1988 and references therein). However, Parada et al. (1988) note there is evidence of partial Ar loss, suggesting the Cogotí Supergroup is likely to be Late Cretaceous to Paleocene in age. Coeval to the Cogotí Supergroup is the extrusive Los Elquinos Formation (69.8 ± 0.9 Ma to 57.6 ± 2.5 Ma (Pineda and Emparan, 2006)) which consists of basaltic to rhyolitic lavas, tuffs and breccias (Charrier et al., 2007). During the Paleocene a number of calderas, including the Tierras Blancas Caldera (Emparan and Pineda, 1999), also formed along the margin between 26 and 30 °S (Charrier et al., 2007). To the east of the volcanic arc, mafic, intra-plate volcanism was concurrent with the emplacement of the Cogotí Supergroup (Litvak and Poma, 2010). The Río Frio Basalts were erupted in what is now the Argentinean Frontal Cordillera and have been K–Ar dated at 55.9 ± 1.9 Ma (Litvak and Page, 2002).

A general reduction in magmatic activity has been identified between ~39 and 26 Ma in the southern Central Andes (Parada et al., 1988), however, some arc magmatism continued during this time interval. The Bocatoma Unit has been dated as Eocene to Early Oligocene with reported Ar–Ar and K–Ar ages ranging between 39.5 and 30 ± 1.9 Ma (Bissig et al., 2001; Martin et al., 1995; Mpodozis and Cornejo, 1988; Nasi et al., 1990). This primarily intrusive unit consists of fine grained to coarsely porphyritic diorites and granodiorites, and some andesitic porphyries (Bissig et al., 2001; Makshev et al., 1984). A number

of dacitic and rhyolitic ignimbrites and lava flows located in the Valle del Cura region (Frontal Cordillera, Argentina) have been K–Ar dated between 44 ± 2 and 34 ± 1 Ma and have been assigned to the Valle del Cura Formation (Limarino et al., 1999; Litvak and Poma, 2005). However, it has recently been suggested that these Eocene to early Oligocene K–Ar ages may be unreliable due to the high levels of hydrothermal alteration evident in these units and new Ar–Ar dating suggests these volcanic sequences are Oligocene to Early Miocene in age (Winocur et al., 2015).

Following the break-up of the Farallón plate and reconfiguration of the margin at ~25 Ma (Lonsdale, 2005), the extensive Doña Ana Group was erupted at and near the arc front, spanning either side of the current Chilean–Argentine border. The Group consists of two formations; the Tilito Formation (27–23 Ma), composed of high-K calc-alkaline andesite lavas and dacitic to rhyolitic ignimbrites, which have been intruded by basic to intermediate dykes; and the Escabroso Formation (21–18 Ma), composed of medium-K, pyroxene bearing, calc-alkaline basaltic and andesitic lavas (Kay et al., 1987, 1991; Makshev et al., 1984; Martin et al., 1997). The Tilito Formation is thought to be derived from a long lived volcanic centre and the volcanic rocks have undergone significant hydrothermal alteration and mineralisation (Bissig et al., 2001; Litvak et al., 2007; Syracuse et al., 2010). The Tilito and Escabroso formations are separated by a major unconformity (Martin et al., 1995) which has been attributed to a period of deformation at ~20 Ma (Kay and Mpodozis, 2002).

During the production of the calc-alkaline Doña Ana Group at the arc front, the Las Máquinas basalts were being erupted in the back-arc region. These alkaline basalts have been K–Ar dated between 22.8 ± 1.1 Ma and 22.0 ± 0.8 Ma and their trace element geochemistry suggests they were erupted in an extensional setting with influence from the subducting slab (Kay et al., 1991; Litvak et al., 2005). The volcanic

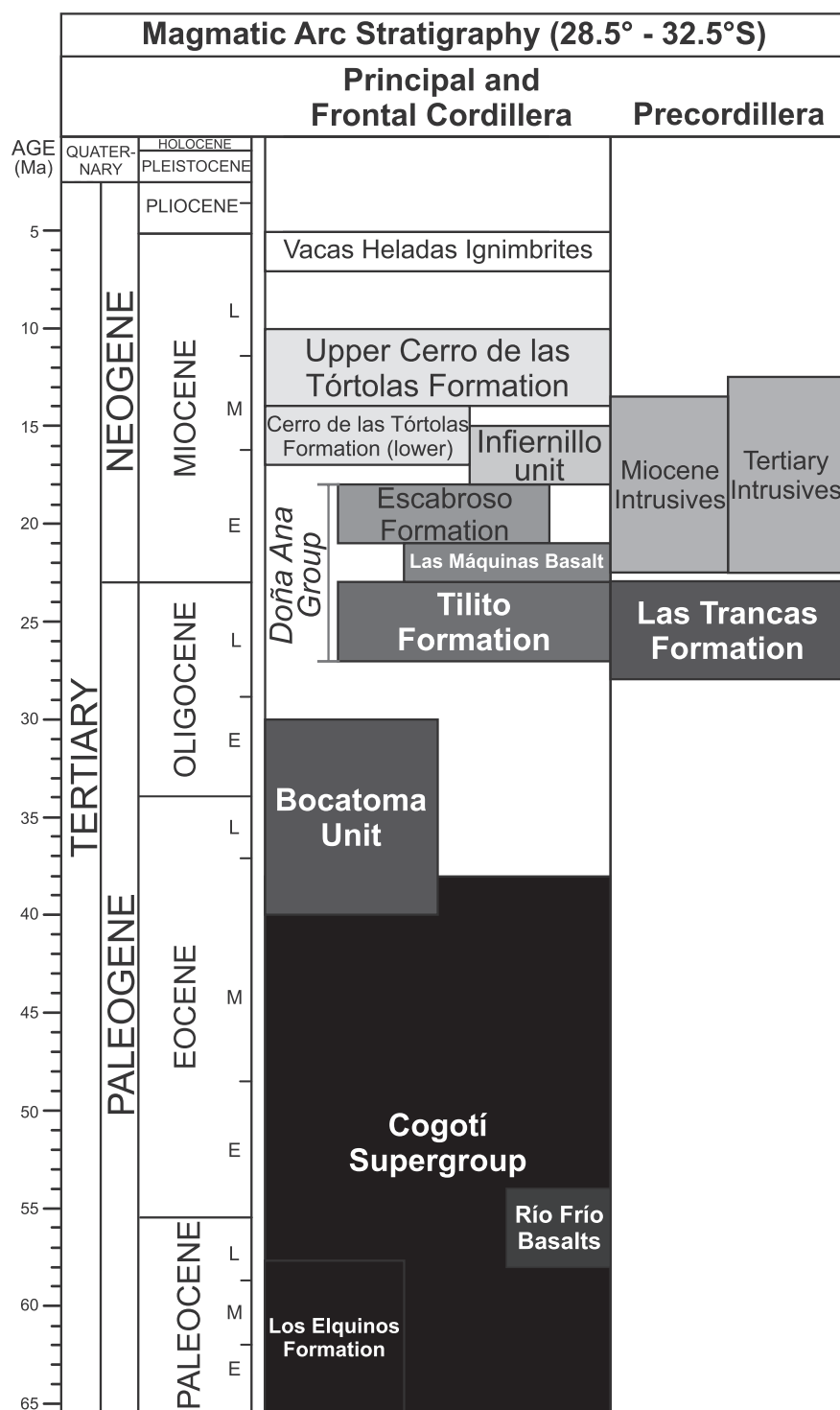


Fig. 2. The Cenozoic magmatic arc stratigraphy of the Principal Cordillera, Frontal Cordillera and Precordillera in the southern Central Andes. References are outlined in the text.

Las Trancas Formation, which outcrops in the Argentinean Precordillera and consists of andesitic to rhyolitic proximal block-and-ash pyroclastic flow deposits, ignimbrites, tuffs and dacitic lava flows, has also been identified as coeval with the Tilito Formation (Poma et al., 2005).

The volcanic Cerro de las Tórtolas Formation also appears on either side of the current Chilean–Argentinean border (Fig. 1). These lavas were erupted during the middle Miocene and are primarily composed of amphibole bearing, medium- to high- K calc-alkaline andesites and dacites. Litvak et al. (2007) and Ramos et al. (1989) identify two separate sequences; an older (17–14 Ma) andesitic to basaltic andesitic

lower section which appears to have been erupted through a normal thickness of crust (30–35 km) and a younger (13–10 Ma) dacitic upper sequence.

The Infiernillo unit (18–15 Ma) is thought to be the subvolcanic equivalent of the Cerro de las Tórtolas Formation and is composed of high-K calc-alkaline, shallow level, intermediate intrusives (Kay et al., 1987) (Fig. 2). A number of sub-volcanic outcrops identified in the Precordillera have been correlated with the Infiernillo Unit and are referred to as the Miocene Intrusives and Tertiary Intrusives (Cardó and Díaz, 1999; Cardó et al., 2007). The Miocene Intrusives which primarily

consist of granitoids and have been dated between 22.4 ± 0.1 and 21.2 ± 0.1 Ma (Llambías et al., 1990). Ages as young as 13.5 ± 7 Ma have been obtained for other deposits (JICA-MMAJ, 1999) and these have also been grouped into the Miocene Intrusives (Cardó et al., 2007). The Tertiary Intrusives consist of sub-volcanic andesites and dacites, and K–Ar dating has given ages of 18.3 ± 2.5 Ma and 17.5 ± 5 Ma (Cardó and Díaz, 1999; Leveratto, 1976), as well as a younger age of 8.8 ± 0.3 Ma (Wetten, 2005).

The Late Miocene, Vacas Heladas Ignimbrites represent the last significant volcanic activity in the region with a reported K–Ar age of 6.0 ± 0.4 Ma (Ramos et al., 1989). These high-K rhyolitic and dacitic tuffs lie unconformably over the Oligocene–Miocene sequences and have been correlated with the Vallecito Formation in Chile, which yields the same age (Bissig et al., 2001; Makshev et al., 1984). These ignimbrites are isotopically enriched and contain the highest proportion of crustal components (e.g., Litvak et al., 2007).

4. The southern Central Andean basement

The basement present in the Principal and Frontal Cordillera's is primarily composed of Paleozoic marine sedimentary deposits and meta-sediments which have been intruded, and unconformably overlain by Late Paleozoic to Mesozoic plutonic complexes and volcanic deposits (Kay et al., 1989; Martin et al., 1999). In Chile, Late Paleozoic–Mesozoic plutonic complexes range in composition from gabbros to granites with two 'super-units' identified according to age: the Late Carboniferous–Early Permian, Elqui Complex and the Permian–Early Jurassic, Ingaguás Superunit (Mpodozis and Cornejo, 1988; Mpodozis and Kay, 1990, 1992; Nasi et al., 1990). The Colangüil Batholith is the age equivalent in Argentina (e.g., Llambías and Sato, 1990, 1995; Sato et al., 2015). There are also extensive deposits of Permian–Early Jurassic silicic, volcanic rocks (e.g., the Choiyoi Group and the Pastos Blancos Group) (Martin et al., 1999; Nasi et al., 1985). All the aforementioned Late Paleozoic–Mesozoic plutonic and volcanic rocks are suggested to have formed in the late stages of Carboniferous to Early Permian subduction along the western margin of Gondwana, and in a more extensional tectonic setting after the cessation of subduction in the Early Permian (Martin et al., 1999; Mpodozis and Kay, 1992).

The basement in the Argentinean Precordillera is composed of Grenville-aged crust (ages between ~1300 and ~950 Ma that are contemporaneous with the North American Grenville province) overlain by Cambrian to Ordovician strata. Although no Grenville-aged basement is exposed at the surface its presence has been identified by various geochemical studies and through the presence of xenoliths and xenocrystic zircon grains in Miocene volcanic rocks (e.g., Abbruzzi et al., 1993; Jones et al., 2015; Kay et al., 1996). It has been suggested that the basement of the Precordillera is a rifted fragment of Laurentian crust which was accreted onto the western margin of Gondwana during the Ordovician (e.g., Astini et al., 1995; Kay et al., 1996; Thomas and Astini, 2003; Thomas et al., 2004), although the origin and the exact timing of rifting and accretion remains widely debated (e.g., Finney, 2007; Keller, 1999; Rapela et al., 1998).

5. Sample preparation and analytical methods

5.1. Sample collection

Representative samples (based on the published maps and formation descriptions of Cardó and Díaz (1999), Cardó et al. (2007), Emparan and Pineda (1999), Mpodozis and Cornejo (1988), Nasi et al. (1990), Pineda and Emparan (2006), Pineda and Calderón (2008)) were collected from each of the major intrusive/extrusive Late Cretaceous to Late Miocene arc formations (detailed in Section 3) present between 29 and 31 °S (Figs. 1 and 2). Due to the eastward migration and expansion of the magmatic arc activity during this time interval, the sample locations form an W–E transect across the Andean Cordillera

from Chile into Argentina (Fig. 1). Late Cretaceous to Late Miocene plutonic and volcanic rocks in the southern Central Andes are typically evolved, but where possible mafic samples were collected in order to evaluate source compositions and processes. A number of Late Paleozoic–Early Mesozoic basement samples were also collected in order to assess their potential role in the contamination of the Late Cretaceous to Late Miocene arc magmas.

5.2. U–Pb dating

In order to obtain zircon grains for U–Pb dating ~5 kg of each sample was crushed using a tungsten carbide jaw crusher. Zircons were then separated from 42 crushed samples using a combination of density and magnetic separation (Section 1, Supplementary Material). Individual zircon grains were hand-picked under a binocular microscope and mounted in epoxy resin accompanied by zircon Geostandards 91500 and/or GJ-1. These epoxy mounts were then ground and polished to expose the interior of the zircons at the surface.

Prior to analysis individual zircon grains were imaged and characterised using a Philips XL30CP Scanning Electron Microscope (SEM) at the University of Edinburgh in order to determine the presence or absence of multiple growth phases, xenocrystic cores, inclusions, and cracks. Imaging was carried out in both secondary electron (SE) and backscatter electron (BSE) modes, and suitable, representative zircons and specific locations for analysis were identified. U–Th–Pb analysis of zircons was performed on a Cameca ims 1270 secondary ion mass spectrometer (SIMS) at the NERC Edinburgh Ion Microprobe Facility (EIMF) using analytical procedures similar to those described by Kelly et al. (2008). Full details of analytical methods, applied corrections and data reduction are outlined in the Supplementary Material. Subsequent to analysis all analysed zircons were imaged on a SEM in both cathodoluminescence (CL) and SE modes to check the exact position of analysis, and to ensure the absence of cracks and inclusions at the bottom of the analysis pits (Fig. 3). Data from any problematic analysis locations (i.e. cracks present) was rejected. A total of 313 successful U–Th–Pb analyses were made and in most cases at least 8 successful analyses of separate zircon grains were made per sample. Multiple analyses (core and rim) were made on selected zircon grains in order to obtain information on growth history and inheritance (Fig. 3).

5.3. Ar–Ar dating

Due to the lack of magmatic zircon in some of the more basic to intermediate samples Ar–Ar dating of plagioclase was conducted on two samples (RJ1111 and AM0887). Plagioclase phenocrysts were separated from the crushed rock samples using similar mineral separation techniques to those used to separate zircon. Plagioclase crystals were hand-picked under a binocular microscope and sent to the Ar–Ar Research Laboratory at the Open University for analysis. Full details are presented in Section 3 of the Supplementary Material.

5.4. Whole-rock major, trace and rare earth element analysis

Sample blocks weighing ~50 g were cleaned and trimmed of any weathered surfaces, veins and xenoliths. These blocks were then crushed into chips using a tungsten carbide jaw crusher. The chips were also checked to ensure they contained no signs of alteration, veins, xenocrystic and xenolithic material, and then powdered in a tungsten carbide TEMA mill to obtain fine, homogeneous powders for analysis by X-ray fluorescence spectrometry (XRF) and inductively-coupled plasma mass spectrometry (ICP-MS). Details are presented in Section 4 of the Supplementary Material.

XRF analyses were carried out in the School of GeoSciences, University of Edinburgh following the analytical methods outlined in Fitton and Godard (2004) and Fitton et al. (1998). Major, minor and selected trace element (TE) compositions of 56 samples were analysed on a

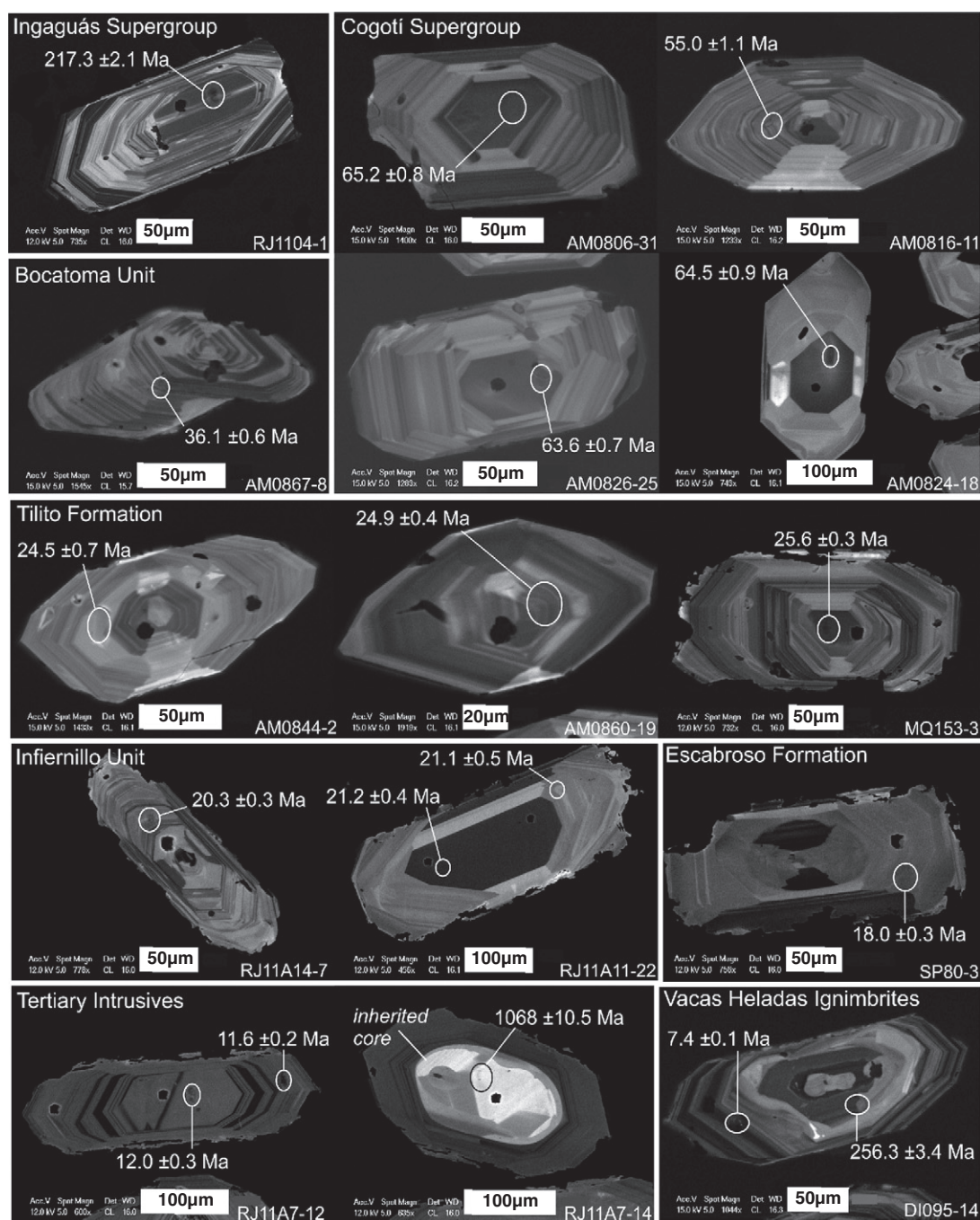


Fig. 3. Cathodoluminescence (CL) images of representative zircon grains from select samples, highlighting the presence of internal growth zoning, inherited cores and the location of SIMS analysis. The U–Pb ages are presented as the $^{206}\text{Pb}/^{238}\text{U}$ ages for the individual zircon grains and the errors are quoted at the 1σ level.

Philips PW2404 wavelength-dispersive sequential X-ray spectrometer with a 4 kW Rh-anode end-window X-ray tube. Major element oxide totals were generally within $\pm 0.9\%$ of 100% and have been recalculated to a 100% volatile free basis. Based on the repeated analysis of an individual sample prepared and analysed five times the precision for the major element analysis is determined as always being $<1.1\%$ (1σ) (Table A4, Supplementary Material). The accuracy of the measurements, based on repeated analysis of standard BHVO-1 (basalt) compared to the published values, is $<3.5\%$ relative (1σ) for all major elements, apart from P_2O_5 where accuracy is 5.5% relative (1σ) (Table A2, Supplementary Material). Precision for the TE and REE concentrations determined by XRF analysis is $<4\%$ (1σ) apart from for Ni where the precision is much lower. This may be a result of the low concentrations of Ni present in

the analysed sample (average = 2.7 ppm). Precision for Ni, based on the repeated analysis of BHVO-1 (117.5 ppm Ni) gave a precision of 0.5% (1σ) (Table A3, Supplementary Material). A full evaluation of the accuracy of the TE and REE analysis is presented in Table A3, Supplementary Material, but is generally determined to be better than 10% relative (1σ).

A subgroup of 39 samples representing each of the major volcanic and plutonic formations were selected for REE analysis via ICP-MS. Select samples were also analysed for U, Th, Pb and Hf concentrations. Sample powders were dissolved using a tri-acid digestion procedure and analysis was carried out on an Agilent 7500ce ICP-MS at the Scottish Universities Environmental Research Centre (SUERC), East Kilbride. Based on the repeated analysis of international standard BCR-2 the

precision of the analysis is <4% (1 σ) and the accuracy is <7% relative (1 σ) for all elements apart from Pb, where precision and accuracy are much lower (7.3 and 30.9% respectively) (Table A6, Supplementary

Material). On this basis the use of Pb in the interpretations will be limited. A good agreement has been found between the TE and REE concentrations produced by XRF and ICP-MS analysis (Figs. A5–A7,

Table 1

The results of U–Pb and Ar–Ar dating and assigned geological unit (determined based on sample location, the new age determinations, and the results of whole rock geochemical analysis). The two sample ages which are displayed in italics and underlined are those obtained by Ar–Ar dating of plagioclase. Sample age calculations have been made using computer program ISOPLOT v3.7 (Ludwig, 2008). The age range ($^{206}\text{Pb}/^{238}\text{U}$ ages) of inherited zircon grains/cores are also presented where identified. The large uncertainty on the U–Pb age obtained for sample AM0890 reflects the limited number of zircon grains obtained from this sample (Supplementary Material). However, the U–Pb age is very similar to the Ar–Ar age produced for sample RJ1111 (61.2 ± 1.0 Ma), which is from the same formation (Los Elquinos Formation).

Sample	Rock type	Age (Ma)	$\pm 2\sigma$ or 95% conf.	Assigned geological unit	Age range ($^{206}\text{Pb}/^{238}\text{U}$, Ma ($\pm 1\sigma$)) of inherited zircon cores/grains
RJ11A18	Granodiorite	280.2	3.5	Plutón Tocota (Colangüil Batholith)	
MQ39	Rhyolite	269.7	2.6	Choiyoi Group	
RJ11A20	Rhyolite	269.6	7	Choiyoi Group	
AM0862	Rhyolite	269.3	5.2	Choiyoi Group	
AM0853	Rhyolite	261.0	6	Pastos Blancos Group	
AM0855	Rhyolite	248.6	5.5	Pastos Blancos Group	
AM0856	Rhyolite			Pastos Blancos Group	
RJ1104	Granite	221.0	4.4	El León Unit (Ingaguás Supergroup)	
AM0812	Diorite	72.6	0.77	Cogotí Supergroup	
AM0823	Granodiorite	69.8	0.73	Cogotí Supergroup	
AM0824	Syeno-diorite	64.6	0.65	Cogotí Supergroup	
AM0806	Granite	64.4	0.66	Cogotí Supergroup	
RJ1103	Syeno-diorite	64.3	0.59	Cogotí Supergroup	
AM0826	Granite	64.2	0.69	Cogotí Supergroup	
AM0819	Diorite			Cogotí Supergroup	
AM0822	Granodiorite	57.3	1.7	Cogotí Supergroup	
AM0814	Diorite			Cogotí Supergroup	
AM0815	Granodiorite	55.0	1.7	Cogotí Supergroup	
AM0816	Granodiorite	54.1	0.76	Cogotí Supergroup	
RJ1101	Granite	38.9	0.99	Cogotí Supergroup	
RJ1109	Diorite			Cogotí Supergroup	
AM0890	Basaltic andesite	61.9	9.11	Los Elquinos Formation	
RJ1111	Basaltic andesite	61.2	1	Los Elquinos Formation	
RF17	Basaltic-Trachyandesite			Río Frío Basalts	
RJ1105	Diorite	40.2	1.2	Tierras Blancas Caldera	
RJ1106	Diorite			Tierras Blancas Caldera	
RJ1107	Basalt			Tierras Blancas Caldera	
AM0867	Andesite	35.6	0.78	Bocatoma Unit	171.8 (± 4.1)
AM0866	Andesite			Bocatoma Unit	
AM0870	Trachy-andesite			Bocatoma Unit	
AM0846	Rhyolite	26.1	1.6	Tilito Formation (Lower Doña Ana Group)	158.0 (± 2.4)
MQ153	Andesite	25.2	0.26	Tilito Formation (Lower Doña Ana Group)	
AM0847	Rhyolite			Tilito Formation (Lower Doña Ana Group)	
AM0845	Rhyolite	24.9	0.32	Tilito Formation (Lower Doña Ana Group)	276.7 (± 2.9)–278.5 (± 2.9)
AM0860	Dacite	24.9	0.4	Tilito Formation (Lower Doña Ana Group)	
ZN122	Andesite	24.8	0.37	Tilito Formation (Lower Doña Ana Group)	
AM0844	Rhyolite	24.7	0.28	Tilito Formation (Lower Doña Ana Group)	241.0 ± 2.7
AM0849	Rhyolite	24.7	0.43	Tilito Formation (Lower Doña Ana Group)	
RF64	Rhyolite	24.3	0.7	Tilito Formation (Lower Doña Ana Group)	388.1 (± 5.3)
PC14	Rhyolite	23.6	0.21	Tilito Formation (Lower Doña Ana Group)	
Z27	Dacite	23.2	0.3	Tilito Formation (Lower Doña Ana Group)	
MQ8	Basalt			Las Máquinas Basalts	
MQ145	Basalt			Las Máquinas Basalts	
RJ11A5	Rhyolite	22.6	0.33	Las Trancas Formation	257.5 (± 2.9)–273.1 (± 3.6)
RJ11A10	Granite	22.2	0.23	Miocene Intrusives	
RJ11A11	Granite	21.4	0.29	Miocene Intrusives	
RJ11A14	Granodiorite	20.4	0.31	Miocene Intrusives	138.1 (± 2.6)
AM0887	Andesite	19.3	0.3	Escabroso Formation (Upper Doña Ana Group)	
1026	Andesite-Trachyandesite	18.2	0.28	Escabroso Formation (Upper Doña Ana Group)	
SP80	Andesite	18.1	0.37	Escabroso Formation (Upper Doña Ana Group)	
AM0886	Andesite			Escabroso Formation (Upper Doña Ana Group)	
MQ158	Basaltic andesite			Escabroso Formation (Upper Doña Ana Group)	
AM0871	Basaltic andesite			Escabroso Formation (Upper Doña Ana Group)	
AM0872	Dacite			Escabroso Formation (Upper Doña Ana Group)	
RF62	Trachyandesite	17.1	0.63	Cerro de las Tórtolas Formation	
RF65	Andesite			Cerro de las Tórtolas Formation	
MQ28	Trachyandesite			Upper Cerro de las Tórtolas Formation	
MQ30	Trachyandesite			Upper Cerro de las Tórtolas Formation	
RJ11A7	Trachyandesite	11.7	0.21	Tertiary Intrusives	1068.1 (± 10.5)–1249 (± 10.9)
RJ11A17	Dacite	9.5	0.18	Tertiary Intrusives	239.7 (± 3.0)–1066.0 (± 13.7)
RJ11A15	Trachydacite	9.4	0.18	Tertiary Intrusives	249.0 (± 2.6)–1225.7 (± 11.7)
MQ33	Rhyolite	6.2	0.19	Vacas Heladas Ignimbrites	15.1 (± 0.2)–255.7 (± 2.7)
DI095	Rhyolite	6.2	0.3	Vacas Heladas Ignimbrites	256.3 (± 3.4)–270.7 (± 3.0)
MQ32	Rhyolite			Vacas Heladas Ignimbrites	
AM0889	Rhyolite			Vacas Heladas Ignimbrites	

Supplementary Material). Therefore, select REE concentrations determined for certain samples by XRF analysis is included alongside the REE concentrations determined by ICP-MS.

6. Results

Detailed sample information, including a summary of the petrology of each formation/unit (Table A7), and full results are presented in the Supplementary Material.

6.1. Geochronological results

The results of U–Pb dating and Ar–Ar dating for individual samples are presented in Table 1. In order to obtain overall U–Pb ages for the Late Cretaceous–Late Miocene samples the data has been plotted on Tera–Wasserburg plots, where the U–Pb data is uncorrected for common Pb and the mixing line is anchored to the $^{207}\text{Pb}/^{206}\text{Pb}$ ratio for modern day common Pb (0.84) (Section 2, Supplementary Material). The overall U–Pb ages for these samples are given by the intercept on the Tera–Wasserburg plot and uncertainties are quoted at the 2σ or 95% confidence level. The overall U–Pb ages presented for the samples of the P–T basement are concordia ages or intercept ages with uncertainties quoted at the 2σ or 95% confidence level (Section 2, Supplementary Material). For the two samples dated using the Ar–Ar dating technique the age determinations are plateau ages with uncertainties quoted at the 2σ level (Figs. A1 and A3, Supplementary Material). All of the plots and age calculations were made using computer program ISOPLOT v3.7 (Ludwig, 2008).

In the majority of cases the new U–Pb and Ar–Ar ages presented in this study confirm the previously reported age range of the sampled geological formations/units. However, in a few instances the ages obtained by this study are at odds with the previously reported ages and the geological maps of the region; these differences are outlined below.

A number of dacitic and rhyolitic ignimbrites and lava flows which outcrop in the Valle del Cura region (Frontal Cordillera, Argentina) have previously produced Eocene K–Ar ages ranging between 44 ± 2 and 34 ± 1 Ma, and have been assigned to the Valle del Cura Formation (Limarino et al., 1999; Litvak and Poma, 2005). Samples of the Valle del Cura Formation collected as part of this study have produced Late Oligocene to Early Miocene ages, ranging between 24.3 and 17.1 Ma (Table 1). Oligocene to Early Miocene ages have also been reported for the Valle del Cura Formation by Winocur et al. (2015). These authors propose that the units previously identified as the Valle del Cura Formation are part of the Doña Ana Group. The U–Pb dating presented by this study supports this inference and some of the samples of the Valle del Cura Formation collected as part of this study have been assigned to the Doña Ana Group. Other samples thought to be the Valle del Cura Formation have been assigned to the Cerro de las Tórtolas Formation due to the younger ages obtained (17.1 Ma) (Table 1, Fig. 2).

A number of intrusive units which crop out in the Precordillera of Argentina have been mapped as Miocene Intrusives and Tertiary Intrusives and correlated with the Infiernillo Unit found on the Chilean side of the border (Cardó and Díaz, 1999; Cardó et al., 2007). However, the U–Pb ages obtained in this study, as well as geochemical evidence, suggest these intrusive bodies are not related. U–Pb ages of between 22.2 ± 0.2 and 20.4 ± 0.3 Ma were obtained for the Miocene Intrusives present in the Llanos del Molle (Llambias et al., 1990) and mapped by Cardó et al. (2007). These ages are significantly older than the ages reported for the Infiernillo Unit on the Chilean side of the boarder ($18\text{--}15$ Ma, (Kay et al., 1987)). Conversely, much younger U–Pb ages (11.7 ± 0.2 to 9.4 ± 0.2 Ma) were obtained for the Tertiary Intrusives which outcrop in the Precordillera. Previously reported K–Ar ages for these sub-volcanic andesites and dacites range between 18.3 ± 2.5 Ma and 17.5 ± 5 Ma (Cardó and Díaz, 1999; Leveratto, 1976), perhaps explaining why these deposits have been linked with the

Infiernillo Unit. The new U–Pb ages presented here are similar to the K–Ar age of 8.8 ± 0.3 Ma reported by Wetten (2005) for the same intrusive bodies, which this particular author refers to as the Cerro Bola Andesite. There is a variety of evidence to suggest that these intrusive bodies have been affected by hydrothermal alteration. On this basis we suggest that some of the K–Ar ages are likely to be unreliable and that the Tertiary Intrusives are Late Miocene in age and consequently distinct from the Infiernillo Unit.

6.2. Geochemical results

6.2.1. Major elements

The results of major oxide analysis are presented in Figs. 4 and 5. The Late Cretaceous to Late Miocene magmatic rocks primarily have medium- to high- K, calc-alkaline compositions. The intrusive samples range from gabbroic to granitic in composition, with SiO_2 contents ranging between 50.9 and 71.3 wt.% (Fig. 4a). The extrusive samples range from basalts to rhyolites with SiO_2 contents ranging between 49.7 and 75.3 wt.% (Fig. 4b). All samples plot within the sub-alkaline field on plots of total alkalis versus silica with the exception of the Paleocene Río Frío Basalt, which is alkaline in composition (Fig. 4b). All the samples are relatively evolved with an average Mg# of 41 and Ni concentration of 11 ppm. The P–T basement rocks have medium- to high-K calc-alkaline to shoshonitic compositions and are more felsic than the Late Cretaceous to Late Miocene arc rocks, with SiO_2 contents ranging between 68.7 and 76.7 wt.% (Fig. 4).

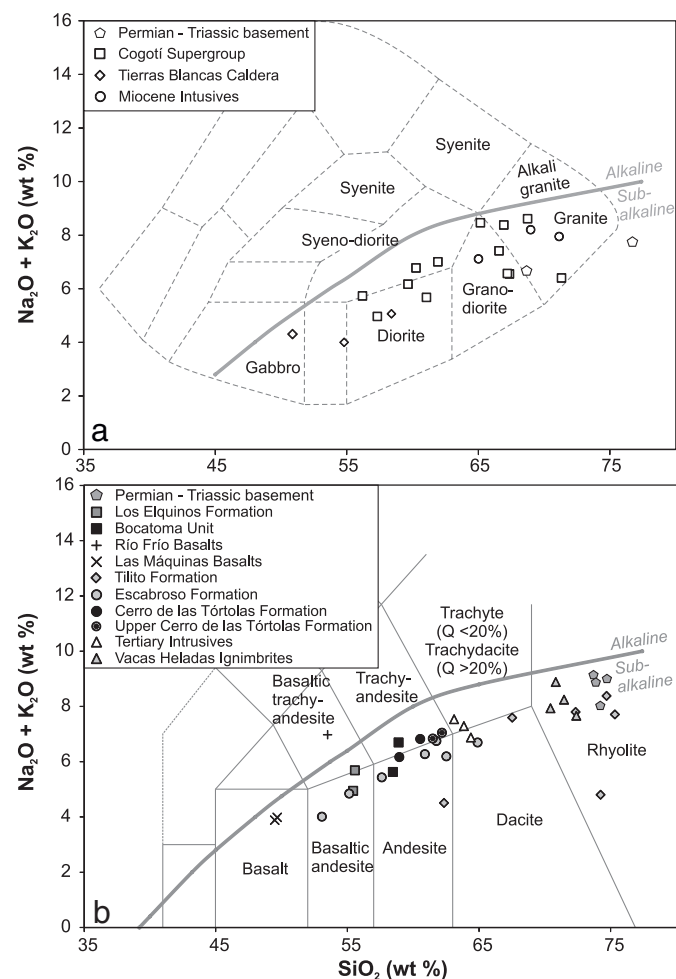


Fig. 4. Plots of total alkalis versus silica content for a) intrusive samples (fields from Wilson (1989)) and b) extrusive samples (fields from Le Maitre et al. (1989)). The alkaline/subalkaline fields are from Irvine and Baragar (1971).

Major elements, TiO_2 , Al_2O_3 , Fe_2O_3 , MgO , CaO , and to a lesser extent MnO display typical negative correlations with SiO_2 content (Fig. 5), whereas K_2O shows a positive correlation (Fig. 5). The plot of P_2O_5 versus SiO_2 content shows a convex trend with a general positive correlation between P_2O_5 and SiO_2 content until SiO_2 reaches ~63 wt.%, after which a negative correlation is observed (Fig. 5). These overall trends

are consistent with fractional crystallisation (FC) processes, for example the increased crystallisation of apatite after ~63 wt.% SiO_2 . The alkali oxides, K_2O and Na_2O show the weakest correlations with SiO_2 (Fig. 5), suggesting that these elements may have been mobilised during alteration. The highest variation is observed in samples of the Cogotí Supergroup which shows a range of K_2O contents between 0.5 to 4.8%

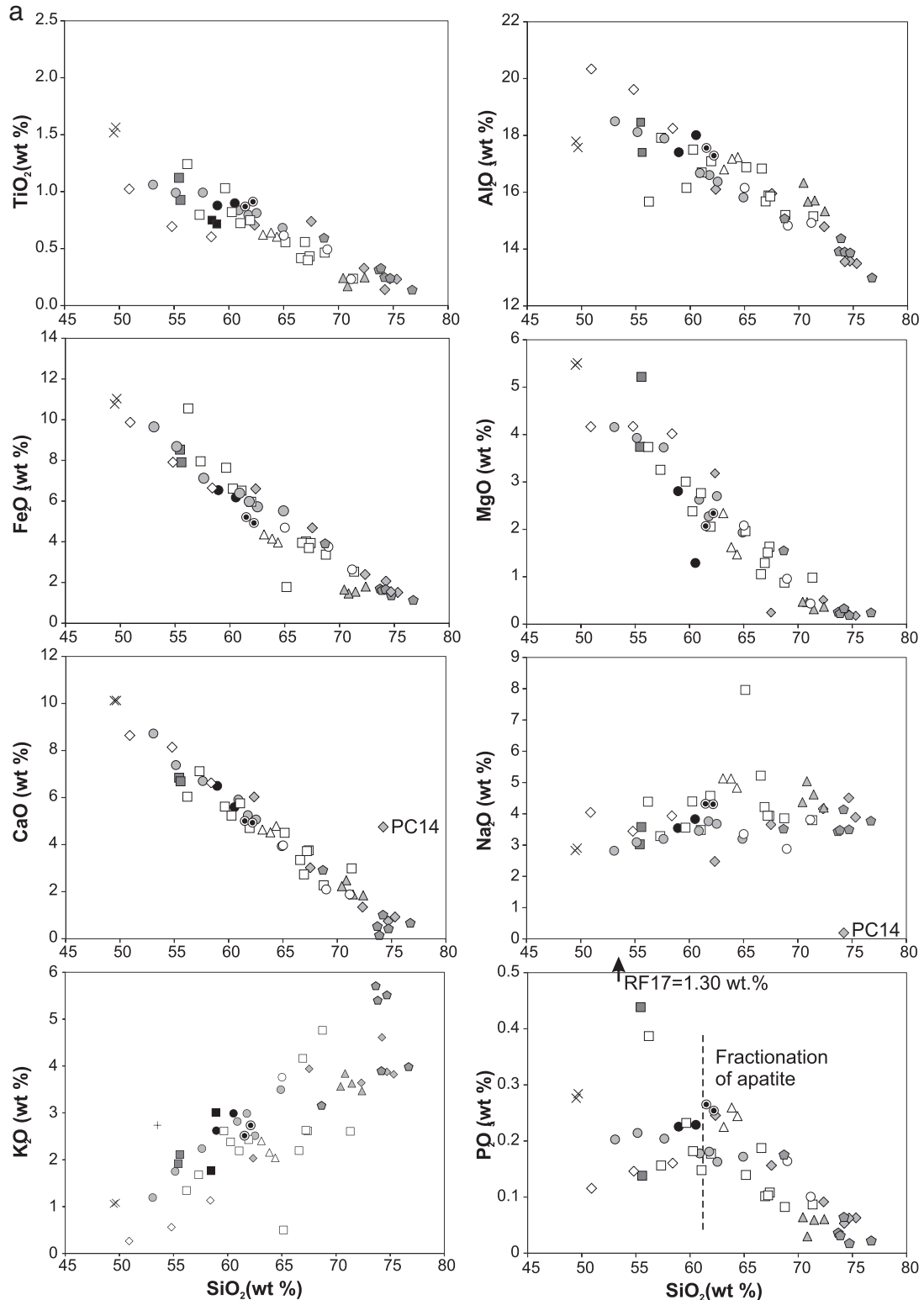


Fig. 5. Harker-type variation diagrams of major (wt.%) and minor (ppm) elements versus SiO_2 content for the Late Cretaceous to Late Miocene samples and the PT basement. Intrusive samples are plotted as open symbols and extrusive samples as filled symbols. The uncertainty on the data points is less than the size of the symbols.

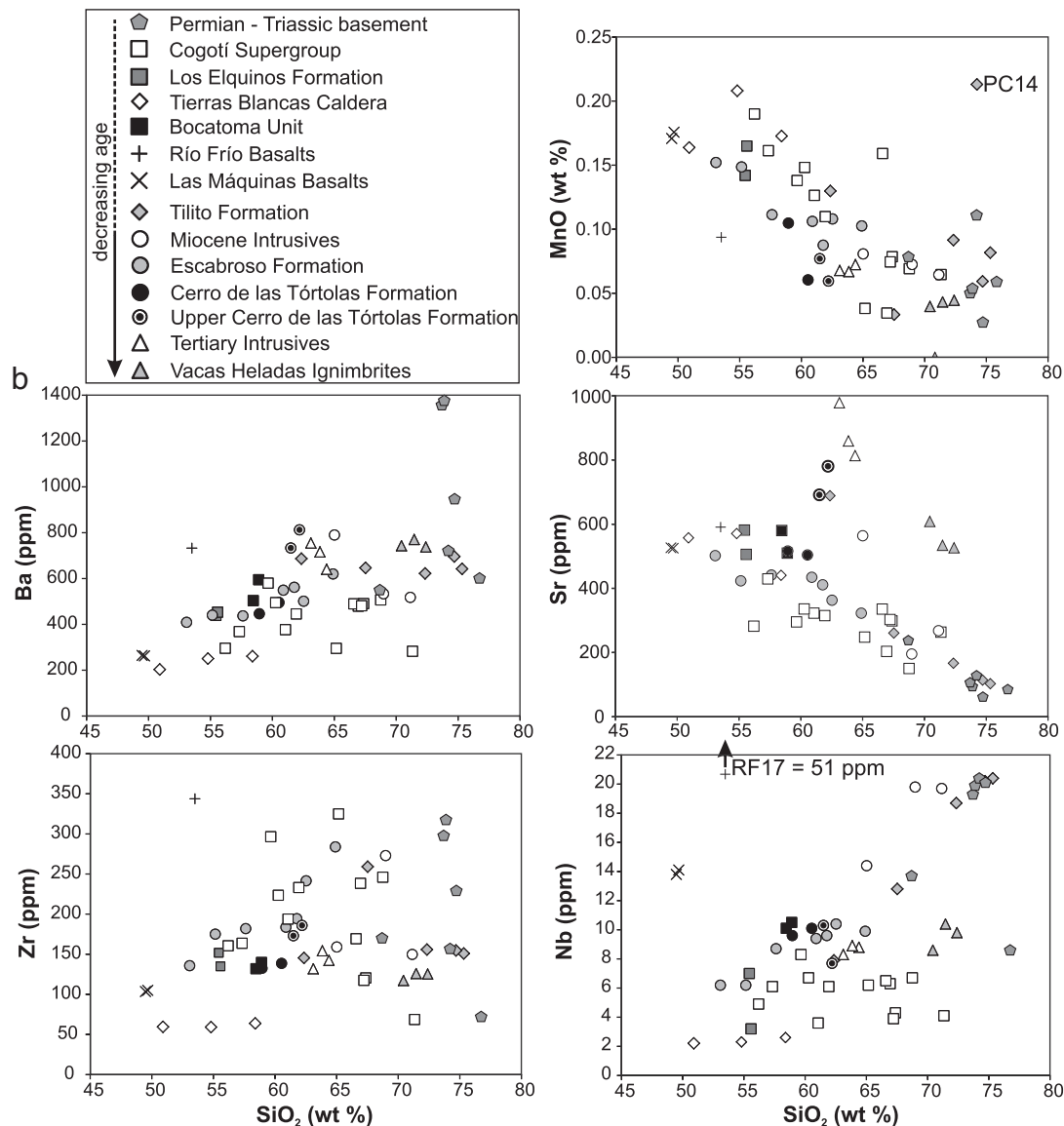


Fig. 5 (continued).

with a limited increase in SiO_2 content. Values for certain major element oxides, obtained for certain samples, also appear to sit away from the main data trends. For example, sample PC14 from the Tilito Formation appears to have lost all of its Na_2O and displays higher CaO and MnO contents (Fig. 5). This suggests leaching of Na, potentially from plagioclase, and replacement with carbonate minerals; this is confirmed by petrographic analysis (Fig. A8, Supplementary Material). Therefore, some variation in the data away from the main trends displayed on the Harker diagrams may be the result of alteration and replacement processes.

6.2.2. Trace elements (TE) and rare earth elements (REE)

The results of trace- and rare earth- element analysis are presented in Figs. 5 and 6. With the exception of the sample (RF17) of the Río Frío Basalts (Paleocene), all samples, including the Las Máquinas Basalts and those of the P-T basement, display typical subduction zone TE and REE signatures with enrichments in the large ion lithophile elements (LILE, e.g., Rb, K, Ba, Sr, Pb) and the light rare earth elements (LREE) relative to the high field strength elements (HFSE, e.g., Nb, Zr, Ti, Y) and heavy rare earth elements (HREE) (Fig. 6). As evident in Fig. 5, sample RF17 (Río Frío Basalts) has a distinct TE composition, with apparent

enrichments in P, Nb and Zr. This sample is also alkaline in composition (Fig. 4b) and is clearly not co-genetic with other Paleocene arc formations (e.g., Cogotí Supergroup and Los Elquinos Formation), indicating that the Río Frío Basalts may have formed from a distinct mantle source.

The multi-element plots for all other samples exhibit prominent negative Nb anomalies and positive K and Pb anomalies (Fig. 6). With the exception of the most mafic sample (MQ8, Las Máquinas Basalts), all samples show negative Ti anomalies and depletions in HREE relative to N-MORB (Fig. 6). The Late Oligocene, Las Máquinas Basalts (MQ8) shows the least enrichment in the LILE, consistent with emplacement in a back-arc setting (e.g., Litvak and Poma, 2010). Samples of the Los Elquinos Formation (Paleocene), Tierras Blancas Caldera (Eocene) and Bocatoma Unit (Early Oligocene) display relatively limited enrichments in LILE, with the exception of Sr. These Paleocene–Early Oligocene samples, along with samples of the youngest (~13–6 Ma) arc formations (Upper Cerro de las Tórtolas Formation, Tertiary Intrusives and Vacas Heladas Ignimbrites), display positive Sr anomalies and limited negative Eu anomalies (Fig. 6). The youngest samples (~13–6 Ma) also have Sr contents which are significantly higher than the overall decreasing trend observed with increasing SiO_2 content (Fig. 5). In addition, these samples display relatively steeply dipping REE patterns with depletions

in the HREE, suggesting a change in the petrogenesis of the youngest arc magmas erupted and emplaced in the southern Central Andes (Fig. 6).

7. Discussion

7.1. Temporal variations in the contamination of southern Central Andean arc magmas

It is clear from many of the TE plots (e.g., Figs. 5b and 6) that there are significant variations in either the degree of melting or the composition of the source of the arc magmas, or in the level of interaction with the continental crust, over time. How the TE compositions have changed over time, due to what processes, and how this relates to the changing geodynamic setting of the southern Central Andean margin, is discussed below.

7.1.1. The Late Cretaceous to Eocene

Concentrations of incompatible, fluid-mobile (e.g., Ba, Pb, U) and fluid-immobile (e.g., Nb, Zr) elements, in the Late Cretaceous–Eocene samples of the Cogotí Supergroup, Los Elquinos Formation, Tierras Blancas Caldera and the Botacoma Unit, remain relatively constant with increasing differentiation (Fig. 5). There are limited correlations

between certain TE ratios and SiO₂ content (Fig. 7) suggesting that these TE variations are not the result of FC. A number of lines of evidence support limited interaction of these arc magmas with the existing continental crust; no inherited zircon grains and cores are identified in these arc rocks (Table 1); ‘mantle-like’ $\delta^{18}\text{O}$ values have been obtained for zircons from these samples (Jones et al., 2015); and low $^{87}\text{Sr}/^{86}\text{Sr}$ isotope ratios have been reported for these the Late Cretaceous–Eocene magmatic belts (Parada et al., 1988). On this basis it is suggested that the observed enrichments in fluid-mobile, incompatible elements (e.g., LILE) and depletions in HFSE and HREE reflect processes occurring in the source region, rather than resulting from crustal contamination and/or differentiation processes.

Overall the fluid mobile/immobile TE ratios (e.g., Ba/Nb, U/Th) are highly variable for the Late Cretaceous–Eocene arc rocks (Fig. 7) suggesting that the source region has been variably influenced by slab-derived fluids. A general increase in these ratios is observed between the Late Cretaceous (~72 Ma) and the Eocene (~50 Ma) suggesting an increased influence of slab-derived fluids on the arc magmas with time (Fig. 8). With an increase in fluid flux from the subducting slab an increase in the amount of partial melting occurring in the mantle wedge might be expected. An increase in certain element ratios (e.g., Nb/Zr, Nb/Yb) between the Late Cretaceous and the Late Eocene

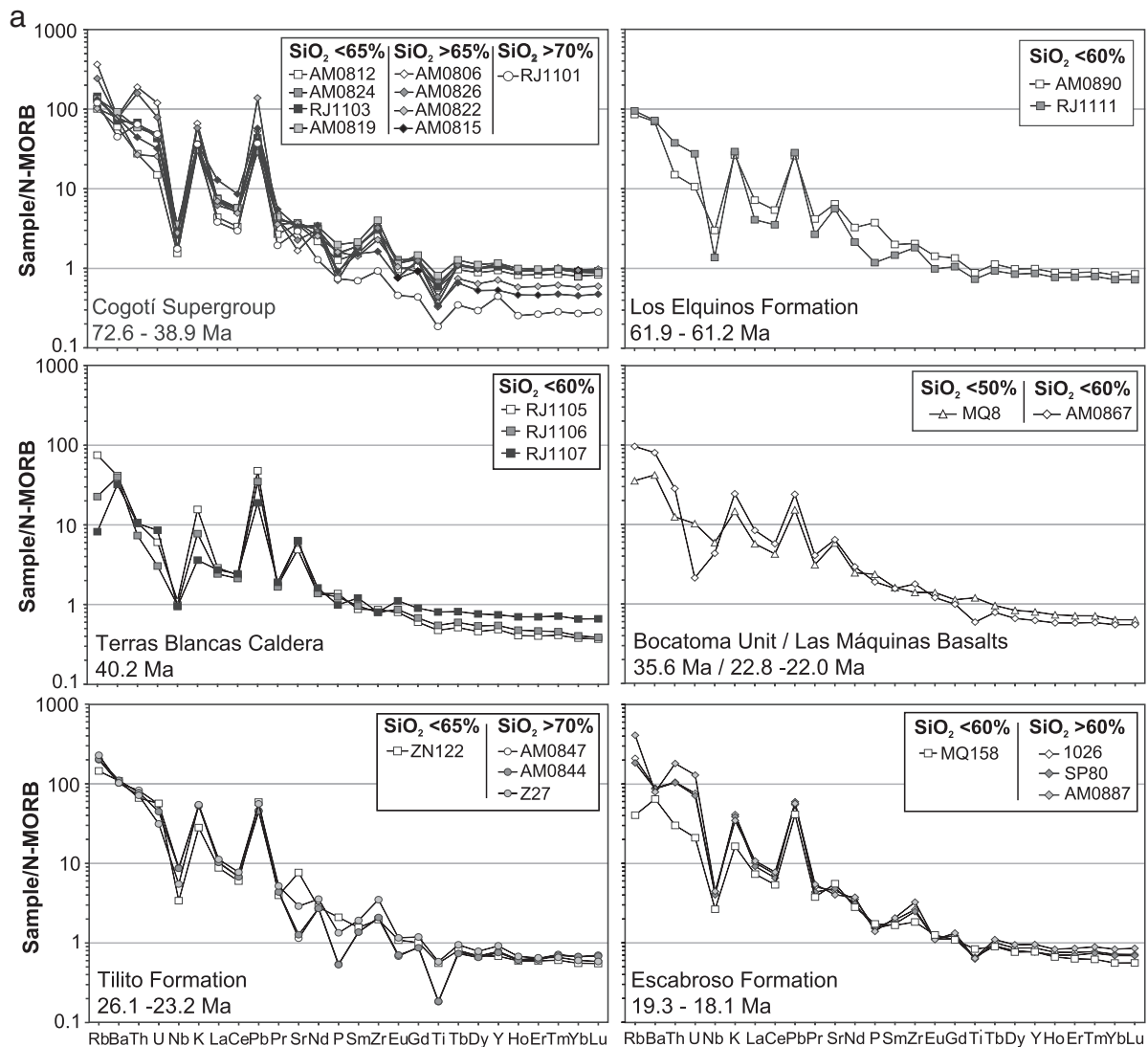


Fig. 6. Multi-element plots normalised to N-MORB values (Sun and McDonough, 1989) for each of the major Late Cretaceous to Late Miocene geological formations/units and the P–T basement.

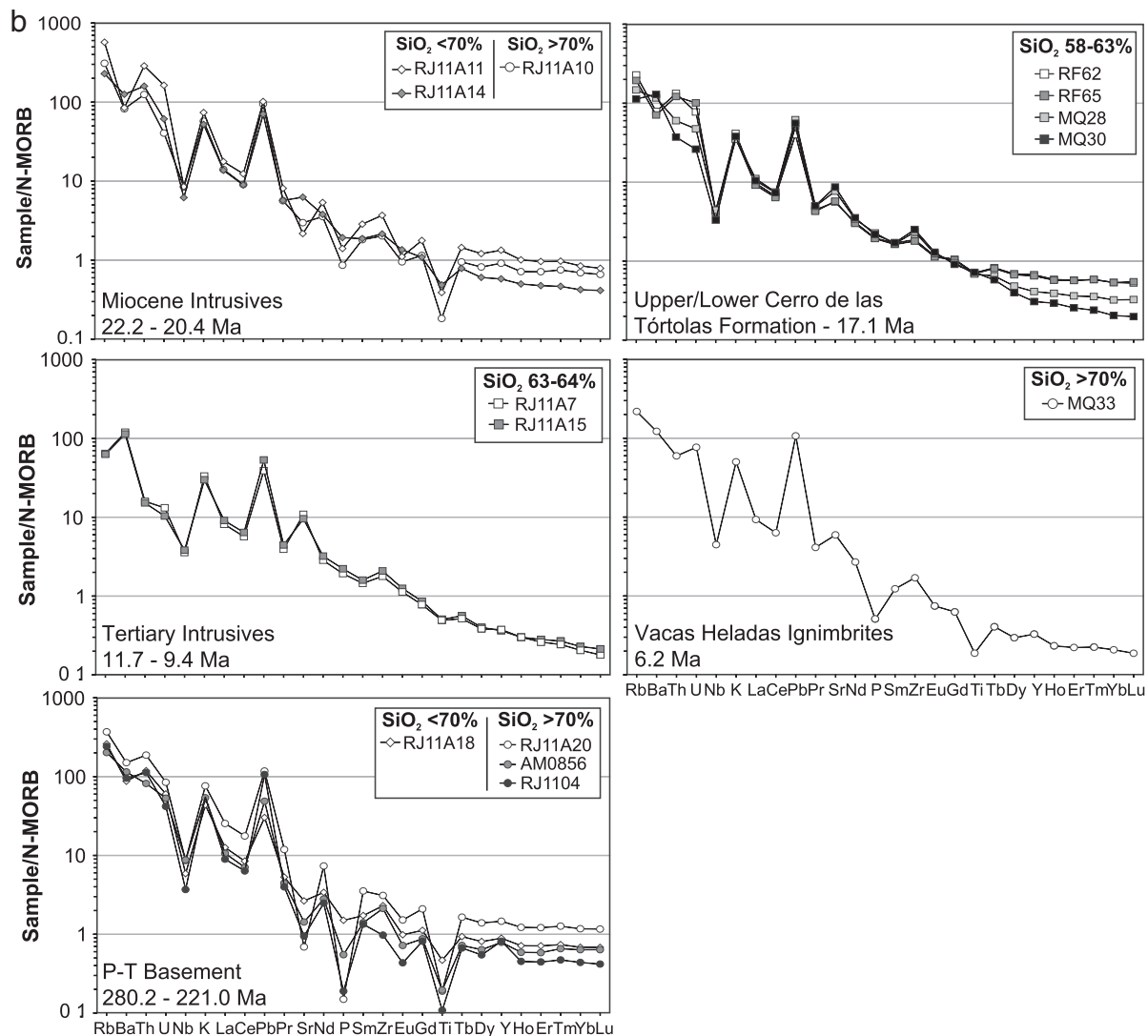


Fig. 6 (continued).

(Fig. 8) could be interpreted as an indication of a decrease in partial melting of the mantle over time. This is at odds with the evidence for an increase in fluid flux from the slab (e.g., increasing Ba/Nb and U/Th (Fig. 8)). Therefore, these element ratios are interpreted as representing an increase in the enrichment of the mantle wedge, either with subduction derived components (e.g., sediments) and/or due to an influx of asthenospheric mantle.

During this time interval magmatism was also occurring in a back-arc position, east of the main volcanic arc. These extension-related basalts (Río Frío Basalts 55.9 ± 1.9 Ma (Litvak and Page, 2002)) have a distinct composition to the magmas erupted in the main volcanic arc. These basalts exhibit high fluid immobile, incompatible TE ratios (e.g., Nb/Zr) and low fluid mobile, incompatible TE ratios (e.g., Ba/Nb), suggesting they represent small degree partial melts which received little influence from slab-derived fluids, as suggested by Litvak and Poma (2010).

7.1.2. The Late Oligocene to Early Miocene

After a period of reduced arc magmatism between the Mid Eocene and the Late Oligocene (Parada et al., 1988, 2007) the Doña Ana Group (Tilto and Escabroso Formations) was erupted at the arc front. The samples of the Tilto Formation (Lower Doña Ana Group) from closer to the trench, have quite distinct compositions from those collected farther to

the east, despite their being of the same age (Late Oligocene). The more westerly rhyolitic ignimbrites (AM0844, AM0846 and AM0847) are highly evolved ($\text{SiO}_2 > 72$ wt.%), have high concentrations of Nb (> 18 ppm) accounting for high Nb/Zr and Nb/Yb ratios (Figs. 8 and 9). The more easterly samples (ZN122 and Z27) are less evolved with andesitic-dacitic compositions.

The presence of inherited zircon cores with P–T ages (ranging between 278.5 ± 2.9 Ma and 241 ± 2.7 Ma, Table 1) in the samples of the Tilto Formation from the Chilean side of the margin, suggests bulk assimilation of the P–T basement (e.g., Beard et al., 2005). It has previously been suggested that the contamination of the Late Oligocene–Early Miocene arc magmas with P–T aged lower crust accounts for the relatively high $^{87}\text{Sr}/^{86}\text{Sr}$ ratios (0.705335) of the Doña Ana Group (e.g., Kay and Abbruzzi, 1996). The range of inherited zircon ages obtained by this study is within the range of U–Pb ages obtained for the Choiyoi Group and Pastos Blancos Group, which comprise part of the basement stratigraphy. These basement groups also appear adjacent to the Tilto Formation in outcrop and therefore it seems likely that the magmas of the Tilto Formation have assimilated this crust. The similar geochemical features (e.g., negative Eu, Ti and P anomalies, positive Y anomalies, high Nb/Zr ratios) observed in samples of the P–T basement and the rhyolitic samples of the Tilto Formation (Figs. 4, 5, and 7) support this suggestion. No inherited zircon cores were found in the

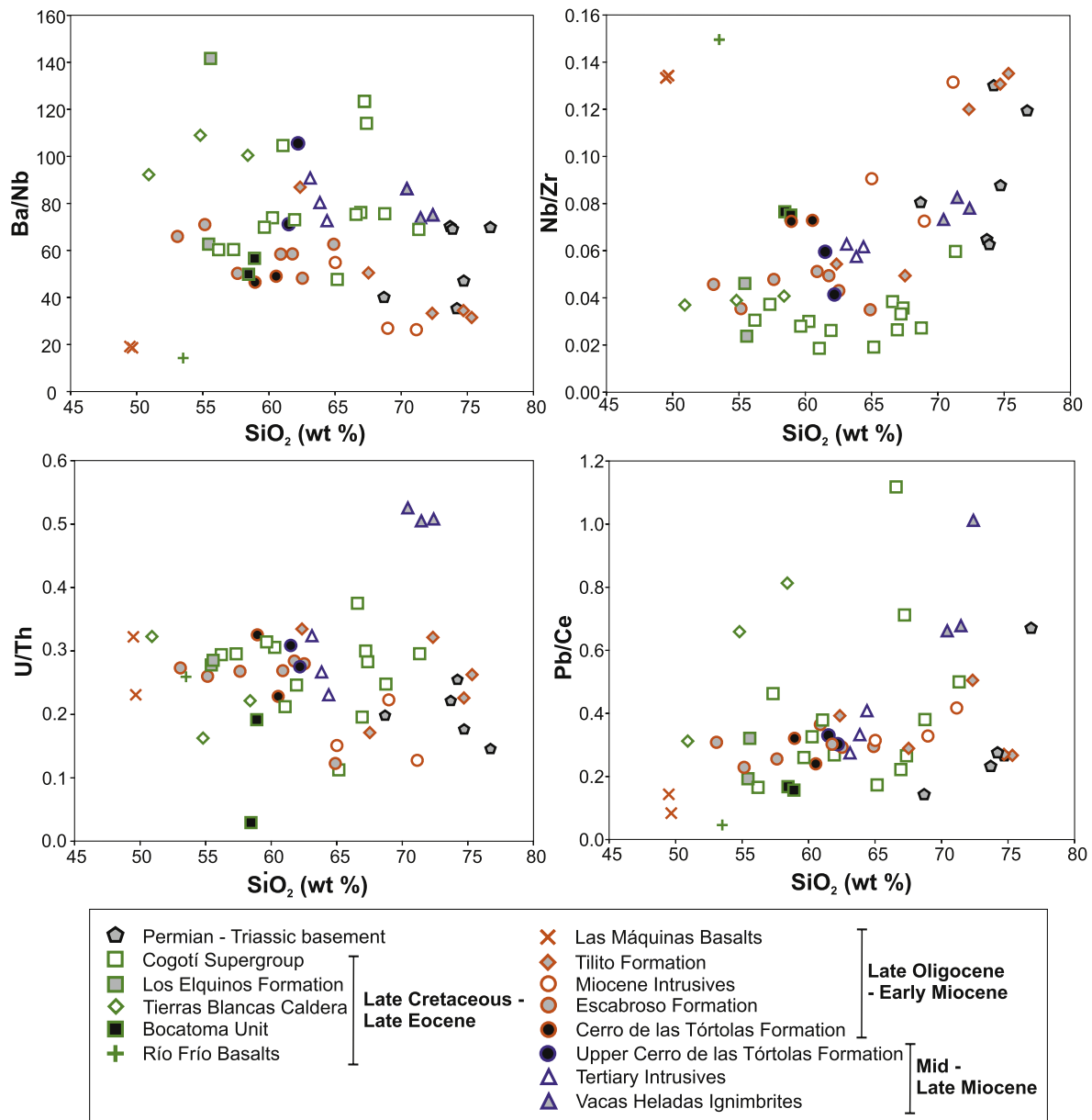


Fig. 7. Ratios of fluid-mobile/immobile incompatible TE (Ba/Nb, U/Th and Pb/Ce) and fluid-immobile/immobile incompatible TE (Nb/Zr) plotted against SiO_2 content.

more mafic samples erupted farther to the east, providing evidence for a more limited interaction between the arc magmas and the basement farther away from the trench.

Coeval with the eruption of the Tilito Formation, the Las Máquinas Basalts were emplaced to the east, on the Argentinean side of the margin. These basalts have high Nb/Zr (Fig. 9) and Nb/U ratios and low fluid mobile/immobile incompatible element ratios (e.g., Ba/Nb and Pb/Nb) (Fig. 7) suggesting a limited influence of fluids derived from the subducting slab and initially relatively small degrees of partial melting. This is consistent with these geological units representing back-arc volcanism (Kay and Abbruzzi, 1996; Kay et al., 1991; Litvak and Poma, 2010). On a plot of Nb/Yb vs. Th/Yb the Las Máquinas Basalt plots between the fields for E-MORB and OIB (Fig. 10) suggesting extraction of small degree melts from a relatively enriched mantle source. This might be expected for a region of the subcontinental mantle which has experienced less partial melting and melt extraction than the mantle situated beneath the main volcanic arc. These compositions are also similar to those of Holocene alkali basalts and trachy-basalts erupted in the back-arc region of the Southern Volcanic Zone (SVZ) (Jacques et al.,

2013). These authors suggest that these back-arc basalts are formed from the melting of enriched Proterozoic subcontinental lithosphere.

The Miocene Intrusives, which consist of Early Miocene granitoids that crop out on the border between the Frontal Cordillera and the Precordillera, are highly enriched in incompatible elements such as Rb, Nb, Th, and Ce, which likely reflects their highly evolved nature. Ratios of fluid mobile/immobile incompatible element ratios are generally low, suggesting the limited influence of fluids on the primary magmas (Figs. 7, 8 and 9). The U–Pb zircon ages presented here for the Miocene Intrusives (22.2 ± 0.23 to 20.43 ± 0.31 Ma) overlap with the ages obtained for the back-arc Las Máquinas Basalts (K/Ar dated between 22.8 ± 1.1 Ma to 22.0 ± 0.8 Ma (Kay et al., 1991; Litvak et al., 2005)). Like the Las Máquinas Basalts, the relatively high Nb/Zr ratios could be indicative of relatively small degree partial melting, which would be consistent with their generation relatively far away from the trench and therefore over a more dehydrated slab.

Geochemical modelling suggests that the compositions of the Miocene Intrusives can be generated from the composition of the Las Máquinas Basalts, by a combination of fractional crystallisation (FC),

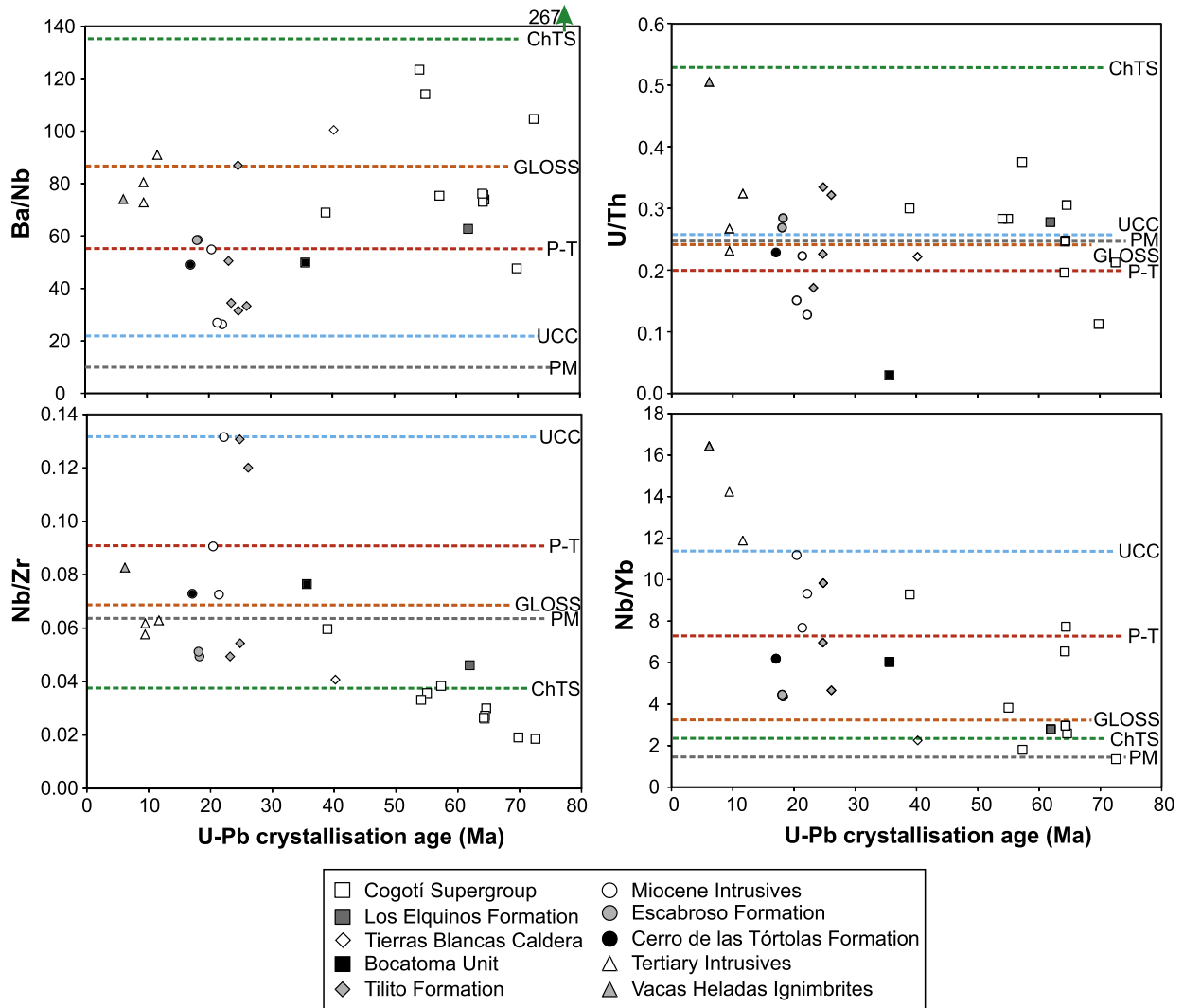


Fig. 8. Plots of fluid-mobile/immobile incompatible element ratios and immobile/immobile incompatible element ratios against corresponding U-Pb crystallisation ages. The values for primitive mantle (PM (Sun and McDonough, 1989)), upper continental crust (UCC (Taylor and McLennan, 1995)), global sediment composition (GLOSS (Plank and Langmuir, 1998)), the composition of sediment currently in the southern Chile trench (ChTS (Jacques et al., 2013)) and the average composition of the P-T basement (this study) are also shown.

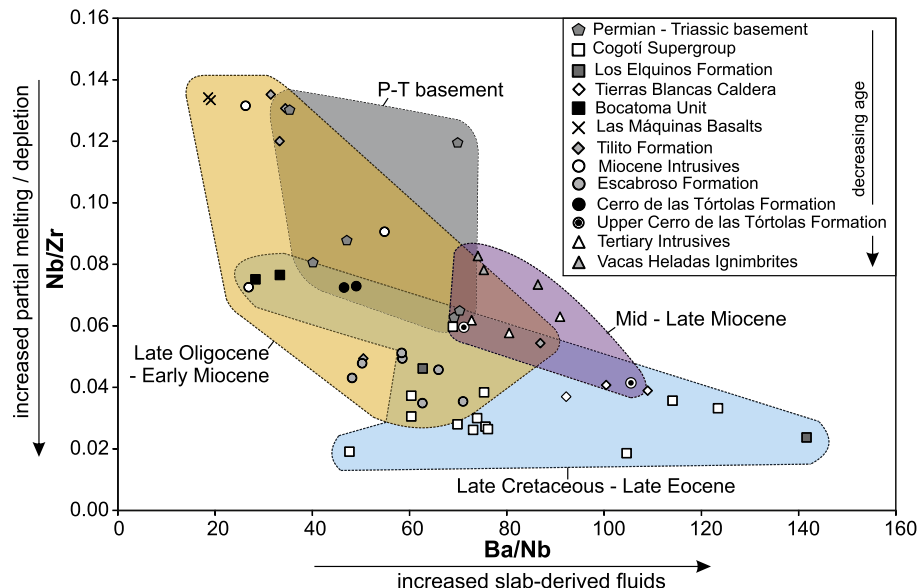


Fig. 9. A plot of Nb/Zr vs. Ba/Nb for the Late Cretaceous to Late Miocene arc magmatic rocks (both intrusive and extrusive), and samples of the P-T basement.

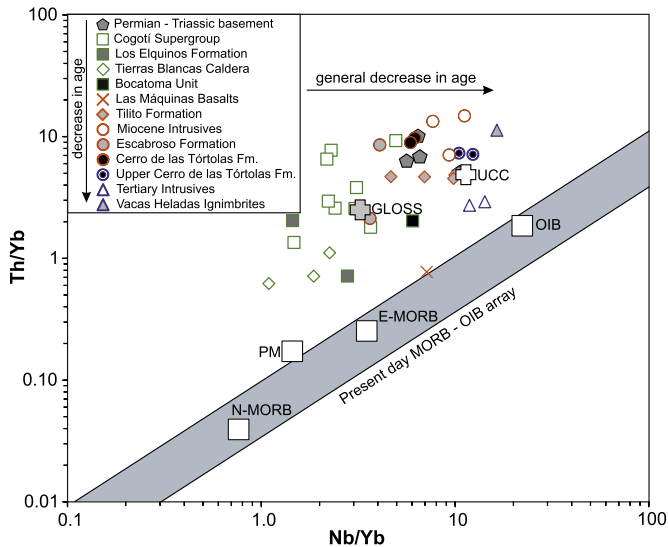


Fig. 10. Th/Yb vs. Nb/Yb discrimination diagram as defined by Pearce (2008). Values for N-MORB, P-MORB, OIB and primitive mantle (PM) from Sun and McDonough (1989), for GLOSS from Plank and Langmuir (1998) and upper continental crust (UCC) from Taylor and McLennan (1995).

and assimilation and fractional crystallisation (AFC) processes involving the P–T basement (Fig. 11), consistent with the presence of inherited zircon in sample RJ11A14 (Table 1). It is difficult to separate the effects of FC from AFC processes, as in this case the fractionating assemblage is virtually the same as the mineral assemblage found in the P–T basement. Evidence from O and Hf isotopic composition of zircon (Jones et al., 2015) suggests that the Miocene Intrusives have also interacted with an ancient, Grenville-aged basement, which is present in the Precordillera. The modelling supports the involvement of this ancient basement terrane, however it is apparent that the majority (~85%) of the assimilated crust must be the P–T basement (Fig. 11). Overall, this suggests that these granitoids, which are located farther away from the trench than the Las Máquinas Basalts, have formed through the differentiation and interaction of these back-arc basaltic melts with the pre-existing Andean crust.

The geochemical modelling also suggests that fractional crystallisation of these basaltic melts can account for the compositions of the less evolved sequences of the Tilito Formation, which outcrop further away from the trench (Tilito Formation – Argentina) (Fig. 11). The more evolved compositions closer to the trench (Tilito Formation – Chile) are more difficult to generate via FC or AFC processes when using the Las Máquinas Basalts as a starting composition. This suggests that the sequences for the Tilito Formation which are closer to the Chilean trench may be the result of decoupled assimilation and fractional crystallisation (i.e. FCA) (Cribb and Barton, 1996) and/or mixing processes involving the P–T basement (Fig. 11), as suggested by the presence of inherited zircon cores. Alternatively they may be derived from a different mantle source, which has received a greater influence from subduction related components.

The extrusive rocks of the younger Escabroso Formation (Upper Doña Ana Group) and Cerro de las Tórtolas Formation (Early Miocene) are generally more mafic than the Late Oligocene samples of the Tilito Formation and Miocene Intrusives (Fig. 4) and have lower Nb/Zr and Nb/Yb ratios, and higher fluid mobile/immobile incompatible element ratios (e.g., Ba/Nb and U/Nb) (Figs. 7, 8 and 9). This suggests a higher degree of partial melting of the mantle wedge due to an increase in fluids derived from the subducting slab, alongside more limited FC and assimilation of the Andean crust. During the Early Miocene (~18 Ma) the JFR began intersecting the Andean margin in this region leading to the initiation of the shallowing of the subducting slab

(e.g., Yañez et al., 2001, 2002). Therefore an increase in the influence of fluids derived from the subducting slab on the source of Early Miocene arc magmas might be expected.

These Early Miocene formations also lack any zircon inheritance (Table 1) providing further evidence for a reduction in the bulk assimilation of the Andean basement in comparison to the Late Oligocene, Tilito Formation and Miocene Intrusives. However, isotopic data still suggests the involvement of some radiogenic crustal components (e.g., Bissig et al., 2003; Jones et al., 2015; Kay and Abbruzzi, 1996; Kay et al., 1991).

7.1.3. The Mid to Late Miocene

During the Mid to Late Miocene the angle at which the Nazca plate was subducting shallowed and as a consequence arc magmatism migrated to the east. During this time interval the Tertiary Intrusives were emplaced in the eastern Frontal Cordillera and the Precordillera. These dacitic to trachydacitic units have relatively low Th, U and Rb concentrations, in addition to HREE depletions (Fig. 6). Kay and Abbruzzi (1996) also identified low Th, U and REE concentrations in the Precordilleran, Miocene arc magmatic rocks and also found them to have the least radiogenic Sr ($^{87}\text{Sr}/^{86}\text{Sr} = 0.7032\text{--}0.7038$) and Pb ($^{206}\text{Pb}/^{204}\text{Pb} = 17.8\text{--}17.9$, $^{207}\text{Pb}/^{204}\text{Pb} = 15.48\text{--}15.49$, $^{208}\text{Pb}/^{204}\text{Pb} = 37.4\text{--}37.5$) isotopic signatures of all the Cenozoic arc magmatic rocks in the Pampean flat-slab segment. They attribute this to the interaction of the Miocene arc magmas with the distinct, Grenville-aged basement present in the Argentinean Precordillera; xenoliths from this basement also yield low Th, U and REE concentrations and unradiogenic Pb isotopic ratios (Abbruzzi et al., 1993). This suggestion is supported by the identification of inherited zircon cores of Proterozoic age in all Tertiary Intrusives samples analysed as part of this study (Table 1).

Kay and Abbruzzi (1996) suggested that the more radiogenic Pb isotopic composition of the Precordilleran Miocene arc magmas in comparison to the Grenvillian xenoliths ($^{206}\text{Pb}/^{204}\text{Pb} = 17.1\text{--}17.8$, $^{207}\text{Pb}/^{204}\text{Pb} = 15.42\text{--}15.49$, $^{208}\text{Pb}/^{204}\text{Pb} = 36.6\text{--}37.4$), requires the interaction of the magmas with an additional component, which has a Pb isotopic composition similar to that with which the Miocene arc magmas in the Frontal Cordillera have interacted. They proposed that this source of radiogenic Pb is derived from the sub-arc mantle wedge. However, in addition to Proterozoic aged inherited cores, this study identified P–T inherited zircon cores in samples of the Tertiary Intrusives (Table 1), thus, suggesting these magmas have also interacted with crust of this age. Radiogenic Pb isotope values (e.g., $^{206}\text{Pb}/^{204}\text{Pb} = 18.44\text{--}18.56$, $^{207}\text{Pb}/^{204}\text{Pb} = 15.65\text{--}15.66$, $^{208}\text{Pb}/^{204}\text{Pb} = 38.38\text{--}38.39$ (Lucassen et al., 2002)) have been determined for the Late Palaeozoic Andean crust, and therefore we propose that the P–T basement may be the source of the radiogenic Pb.

In general as the subducting Nazca plate shallowed the volcanic front expanded and migrated to the east over the course of the Miocene. However, the youngest arc rocks in the region, the Vacas Heladas Ignimbrites occur in the Frontal Cordillera. During the same time interval magmatism was occurring at the Pocho volcanic field in the Sierra de Córdoba, situated directly to the east and 700 km away from the Chile trench. The Pocho volcanic rocks are thought to be associated with the arrival of the shallowly dipping subducting slab under this part of the South American continent (e.g., Kay and Gordillo, 1994). From this it can be inferred that very little of the mantle wedge must have remained under the Frontal Cordillera. Therefore, it is likely that the Vacas Heladas Ignimbrites represent small volume lower crustal melts, generated due the influence of heat and fluids derived from the subducting slab. These volcanic deposits have the highest fluid-immobile, incompatible TE ratios (e.g., Nb/Zr and Nb/Yb (Fig. 8)) of the Mid–Late Miocene arc formations (i.e., 15–6 Ma), suggesting they represent small degrees of partial melting, consistent with the small volumes of erupted magma. The high ratios of fluid-mobile/immobile incompatible TE (e.g., Ba/Nb, Pb/Ce) obtained from the Vacas Heladas Ignimbrites compared to the other Mid to Late Miocene arc magmas, are also indicative of a high

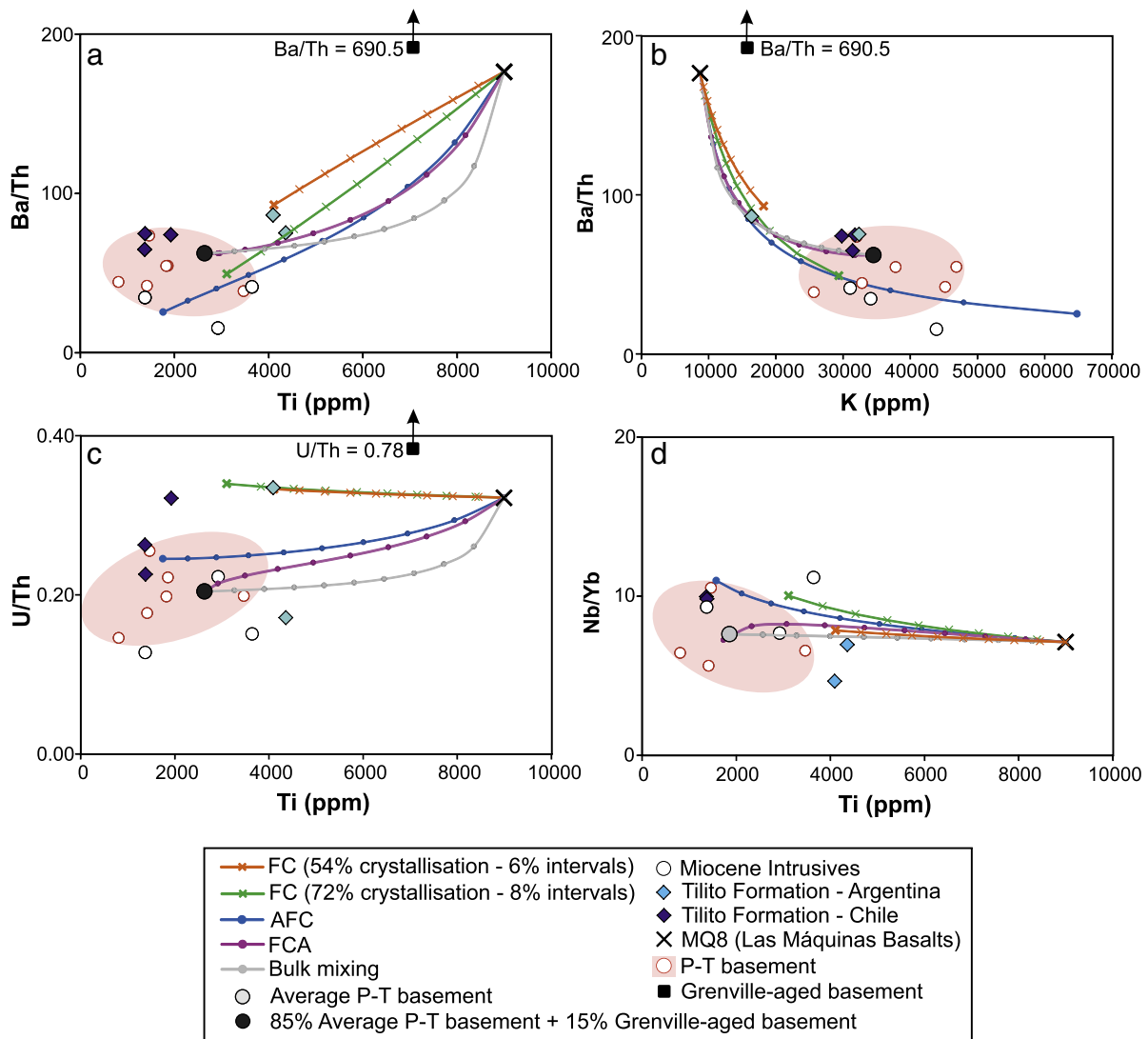


Fig. 11. Geochemical modelling conducted using the FC-AFC-FCA modeler of [Ersay and Helvacı \(2010\)](#). The modelling uses the partition coefficients for intermediate melt compositions and an 'r' value of 0.3 (i.e., 30% assimilated material), as is supported by evidence from zircon isotope data ([Jones et al., 2015](#)). The starting composition used is sample MQ8 (Las Máquinas Basalts) and is the least evolved sample from the region with a composition close to E-MORB ([Fig. 10](#)). The fractionating assemblage used to model the orange FC trend is plagioclase (35%), K-feldspar (15%), magnetite (20%), amphibole (5%), biotite (10%), clinopyroxene (10%) and olivine (5%); consistent with the minerals present in samples of the Las Máquinas Basalts and the more mafic samples for the Tilito Formation which outcrop in Argentina (i.e., further away from the trench) (Table A7, Supplementary Material). In this case increments represent 6% and crystallisation ends at 54%. The fractionating assemblage used to model the green FC trend is plagioclase (30%), K-feldspar (15%), magnetite (15%), amphibole (15%), biotite (13%), clinopyroxene (5%), olivine (5%), apatite (1%) and zircon (1%); consistent with the minerals present in samples of the Las Máquinas Basalts and Miocene Intrusives (Table A7, Supplementary Material). Increments on the green FC, AFC, FCA and mixing lines represent 8% and crystallisation ends at 72%, consistent with what might be expected for granitic (Miocene Intrusives) and rhyolitic rock types (Tilito Formation – Chile). The composition of the Grenville-aged basement is the average composition of xenoliths presented in [Kay et al. \(1996\)](#).

influence of slab-derived fluids on these magmas. These melts have subsequently been contaminated with the Late Paleozoic–Early Mesozoic basement and the older Cenozoic arc rocks, present in the upper crust. This is consistent with TE signatures obtained for the Vacas Heladas Ignimbrites; relatively high incompatible TE ratios ([Figs. 7, 8, and 9](#)) could be indicative of either relatively small degree partial melts and/or assimilation of the continental crust. This is also consistent with isotopic evidence; increasing $^{87}\text{Sr}/^{86}\text{Sr}$ ratios correlate with decreasing ϵNd values between the Late Oligocene and the Late Miocene, with the highest $^{87}\text{Sr}/^{86}\text{Sr}$ ratios (0.7055) and lowest ϵNd values (–2.0) reported for the Vacas Heladas Ignimbrites, suggesting an increase in crustal contamination with time ([Kay and Abbruzzi, 1996](#); [Kay et al., 1991](#); [Litvak et al., 2007](#)). Inherited zircon cores of P–T and Miocene age identify the crustal material being incorporated into the melts ([Table 1](#)).

The Mid to Late Miocene arc magmatic rocks also have adakitic signatures ([Fig. 12a](#)). Diagnostic geochemical features of adakites and their mode of formation remain controversial (e.g., [Castillo, 2012](#)). Originally it was proposed that adakites formed from the partial melting of young (<25 m.y.), basalt crust being subducted beneath volcanic arcs, where garnet and amphibole are residual phases ([Defant and Drummond, 1990](#); [Kay, 1978](#)). Subsequently a number of other mechanisms of producing arc rocks with adakitic signatures have been outlined, including partial melting of a mafic lower crust (e.g., [Chung et al., 2003](#); [Kay et al., 1991, 2005](#)), and high-pressure fractional crystallisation of hydrous mafic arc magmas (e.g., [Castillo et al., 1999](#); [Macpherson et al., 2006](#); [Rodríguez et al., 2007](#); [Rooney et al., 2011](#)). To the south of the study area (~32 °S), [Reich et al. \(2003\)](#) propose that melting of young, hotspot-derived rocks associated with the JFR has resulted in the adakitic signatures of Late Miocene (~10 Ma) intrusions,

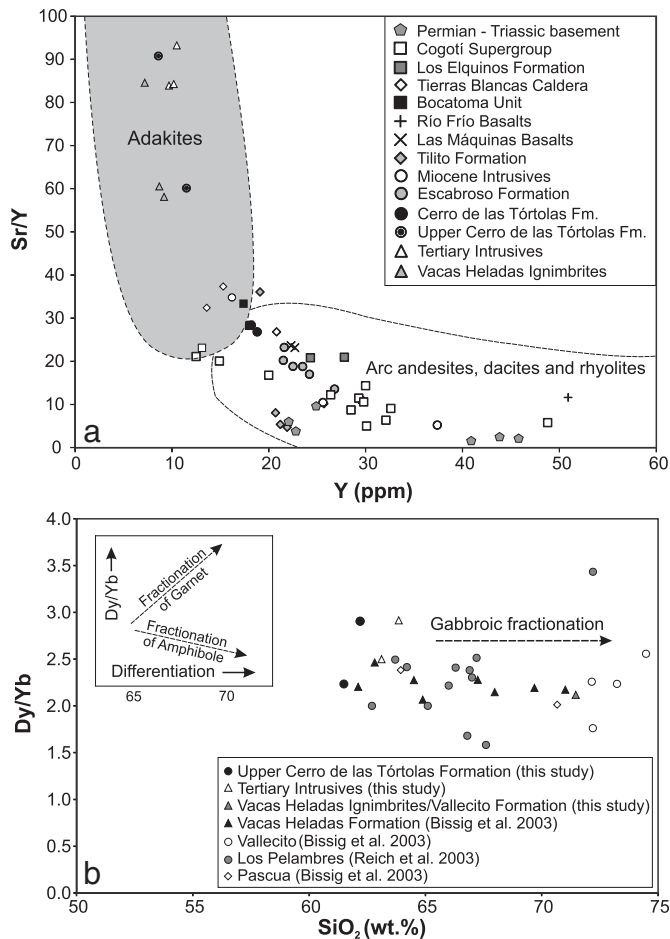


Fig. 12. a) Sr/Y vs. Y (boundaries are from Richards and Kerrich (2007)), typically used for distinguishing adakites as defined by Defant and Drummond (1990) and Drummond and Defant (1990), and b) Dy/Yb vs. SiO₂ (wt.%) for Mid to Late Miocene samples from the Central Andes. Data presented is from this study and from Bissig et al. (2003) and Reich et al. (2003).

on the basis of limited crustal thickness (<35 km at 10 Ma) at these latitudes, combined with the non-adakitic signatures of more recent arc rocks.

In the Pampean flat slab segment it is proposed that the adakitic signatures are the result of the arc magmas equilibrating with high pressure mineral assemblages, including garnet, in the lower crust (e.g., Bissig et al., 2003; Goss et al., 2011; Kay et al., 2005; Litvak et al., 2007). During this time interval the thickness of the continental crust is suggested to have increased to >45 km as a result of crustal shortening (e.g., Allmendinger et al., 1990; Kay et al., 1991). This increase of crustal thickness could have also resulted in the high-pressure fractional crystallisation of garnet or amphibole from the mafic arc magmas (e.g., Davidson et al., 2007; Macpherson et al., 2006). However, the relatively flat trend displayed on a plot of Dy/Yb against SiO₂ content (Fig. 12b) suggests these phases were not fractionated from the melts and that they underwent gabbroic fractionation, which has a limited effect on the shape of REE patterns. This provides further evidence to suggest that the Mid to Late Miocene arc magmas were equilibrating with high pressure mineral assemblages in the lower crust. Overall, the development of adakitic signatures in the Mid to Late Miocene suggests that over the course of the Late Cretaceous to Late Miocene the arc magmas generated were equilibrating with different residual mineral assemblages, with a development from lower pressure assemblages (i.e. pyroxene) to higher pressure assemblages (i.e. garnet), likely reflecting the significant increase in crustal thickness over time.

8. The geodynamic evolution of the southern Central Andes

The new geochronological and geochemical data obtained by this study provides new evidence with which to refine the tectonic and geodynamic models of the Pampean flat-slab segment. An updated evolutionary model for the southern Central Andean margin between the Late Cretaceous and the Late Miocene is outlined below and in Fig. 13.

8.1. The Late Cretaceous–Early Eocene (~75–51 Ma)

During the Late Cretaceous–Early Eocene (~75–51 Ma) the magmatic arc along the western margin of South America was somewhat different to the compressional Andean arc now in existence (Fig. 13a). The oblique angle of subduction and the low convergence rates between the Farallón and South American plates are thought to have caused extension along the margin (Charrier et al., 2007; Pardo Casas and Molnar, 1987; Somoza, 1998). The Late Cretaceous to Early Eocene magmatic rocks, associated with extension, primarily consist of north–south trending plutonic belts. Volcanic rocks associated with these extensive plutonic belts are scarce and may have been removed by erosion.

TE signatures suggest the Late Cretaceous to Early Eocene arc magmas, emplaced in the Principal and Frontal Cordillera's, formed in a subduction zone setting from the partial melting of a metasomatised mantle wedge, which has been variably influenced by slab-derived fluids. Evidence from boron isotopic compositions suggests these fluids were primarily derived from the dehydration of altered oceanic crust and serpentinite (Jones et al., 2014). TE signatures, such as low overall Nb/Zr and Nb/Yb (Figs. 7 and 8), suggest significant partial melting of the mantle wedge took place during this time period. Whole-rock rare earth element geochemistry (e.g., La/Yb ratios) suggests the Late Cretaceous to Early Eocene mantle-derived melts underwent equilibration with/fractional crystallisation of a gabbroic assemblage, suggesting migration of the arc magmas through a crust of normal thickness (~30–35 km). A lack of zircon inheritance, 'mantle-like' oxygen isotope values and juvenile initial εHf values obtained for magmatic zircon (Jones et al., 2015), and low initial ⁸⁷Sr/⁸⁶Sr ratios reported for these plutonic belts (Parada et al., 1988), suggests minimal contamination by older continental crust. This combined evidence suggests that this time period represents a sustained period of upper crustal growth in the southern Central Andes (Fig. 13a).

8.2. The Early Eocene to Early Oligocene (~50–27 Ma)

This time period is characterised by a reduction in arc magmatism and a transition from the emplacement of primarily plutonic belts in the Principal Cordillera, to arc volcanism further away from the subduction zone trench in the Frontal Cordillera (Fig. 13b). During the Mid to Late Eocene granitoids and andesitic porphyries were emplaced in the Principal Cordillera, along with a number of intrusions related to caldera formation. In the Frontal Cordillera volcanic deposits were emplaced (e.g., the Botacoma Unit) and incompatible TE ratios (e.g., Ba/Nb, Nb/Zr) suggest these deposits were formed from small degree partial melting of the mantle wedge, with less influence from slab-derived fluids, in comparison to the plutonic belts present in the Principal Cordillera. The more limited influence of slab-derived fluids may reflect the position of this part of the arc further away from the trench, over a more dehydrated slab (Fig. 13b). An increase in the influence of crustally derived material on the compositions of these arc magmas is also identified between the intrusions emplaced in the Principal Cordillera, and the arc magmas erupted in the Frontal Cordillera. In particular, the presence of inherited zircon suggests that these Frontal Cordillera arc magmas assimilated Late Palaeozoic–Early Mesozoic basement.

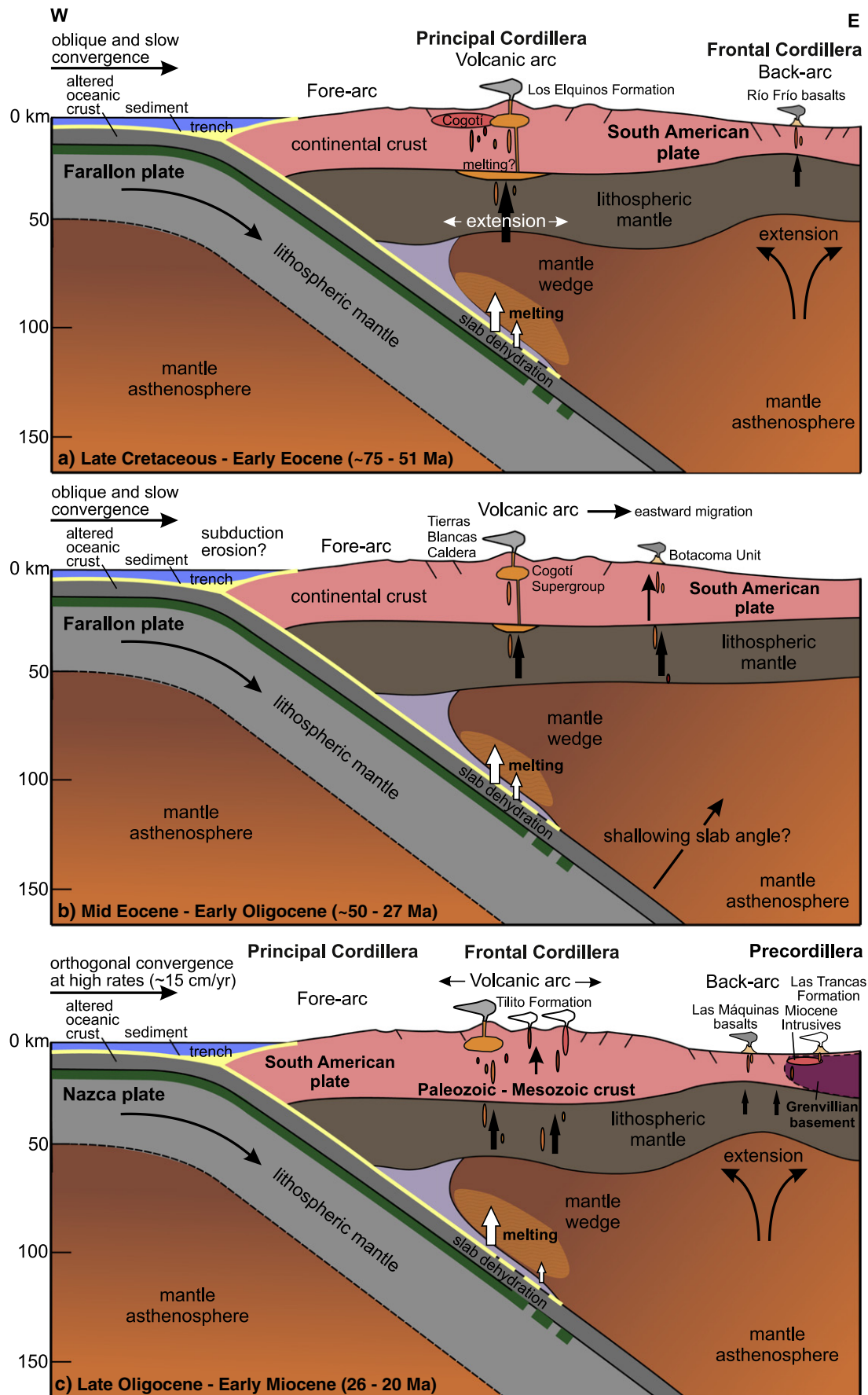


Fig. 13. Schematic cross sections of the southern Central Andean margin at approximately 29–31°S, showing the geodynamic evolution of the margin from the Late Cretaceous (~75 Ma) (a) through to the Late Miocene (6 Ma) (e).

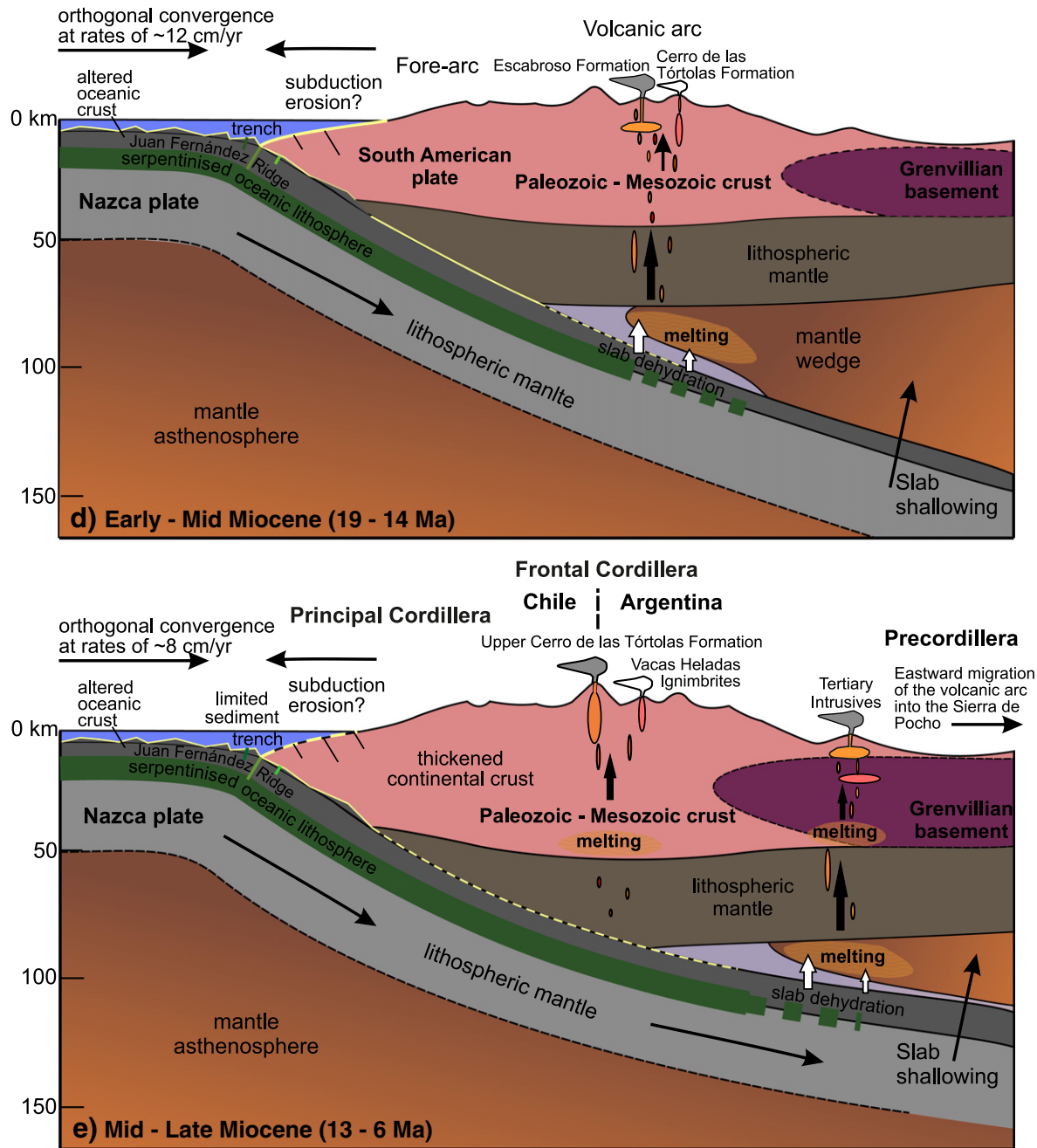


Fig. 13 (continued).

The poor development of the magmatic arc from 50 to 27 Ma may be related to the low convergence rates (~5–8 cm/yr) and oblique angle of subduction (NE direction) operating between the oceanic Farallón and the South American plate (e.g., Pardo Casas and Molnar, 1987; Somoza and Ghidella, 2012). The reduction in arc magmatism has previously been linked with an earlier period of flat-slab subduction along the Central Andean margin (e.g., O'Driscoll et al., 2012). The apparent eastward migration of the arc during this time interval supports the shallowing angle of subduction, however there is little other evidence to support flat-slab subduction during this time interval. For example, La/Yb ratios suggest that the ascending arc magmas were equilibrating with/fractionating a mineral assemblage which reflects a continental crust of normal thickness (~30–35 km), and that these melts were not derived from the melting of the subducting slab, which might result from flat-slab subduction (Gutscher et al., 2000a).

8.3. The Late Oligocene–Early Miocene (~26–20 Ma)

After the period of relative magmatic quiescence, this time interval is associated with a dramatic increase in magmatic activity and a broadening of the magmatic arc (Charrier et al., 2007 and references therein; Pilger, 1984). This has been related to a major change in plate configuration at ~25 Ma involving the break-up of the Farallón plate into the Cocos and Nazca plates (Lonsdale, 2005). This tectonic reconfiguration resulted in subduction becoming more normal to the margin (ENE direction) and convergence rates increasing from ~8 cm/yr to an average of ~15 cm/yr (Pardo Casas and Molnar, 1987; Somoza, 1998; Somoza and Ghidella, 2012).

In the southern Central Andes, this time period is characterised by the eruption of the Tilito Formation (Lower Doña Ana Group) in the main Andean arc, and extension related magmatism in the back-arc

region (Fig. 13c). The Tilito Formation (26.1–23.2 Ma) was erupted over a wide arc front, which is now situated in the Frontal Cordillera. An extensional regime operated to the east of the arc front, both during the late stages, and after the eruption of the Tilito Formation. This back-arc magmatism involved the eruption of the Las Máquinas Basalts (22.8–22.0 Ma (Kay et al., 1991; Litvak et al., 2005)) in the Frontal Cordillera, and the emplacement of high-K granitoids (Miocene Intrusives, 22.2–20.4 Ma) alongside dacitic to rhyolitic ignimbrites and lavas (Las Trancas Formation, 22.6 Ma), in the Argentinean Precordillera. Between ~23 and 21 Ma there is an apparent reduction in magmatism at the arc-front, with magmatic activity concentrated in the back-arc region.

TE signatures and the presence of inherited zircon grains/cores in the high-K, calc-alkaline rhyolites of the Tilito Formation erupted closest to the trench suggests the magmas bulk assimilated the Late Paleozoic–Early Mesozoic basement en route to the surface. The generally more mafic (andesitic) units of the Tilito Formation, erupted further away from the trench, show evidence for a more limited interaction with the Andean basement. The interaction of ascending mantle-derived melts with the overlying Andean continental crust is generally higher in the Late Oligocene to Early Miocene, than is evident earlier (i.e., Late Cretaceous–Mid Eocene). This evidence suggests the Late Oligocene to Early Miocene represented a period of significant crustal reworking and growth of the upper Andean continental crust due to both arc-related, and extension-related magmatism.

8.4. Early–Mid Miocene (~19–14 Ma)

After the apparent reduction in arc magmatism between ~23 and 21 Ma, arc magmatism at the arc-front was reinitiated with the eruption of the basaltic andesite and andesite lavas of the Escabroso Formation (Upper Doña Ana Group) and the Cerro de las Tórtolas Formation. An eastward migration of the arc-front is observed with the majority of arc volcanism occurring on the now Argentinean side of the margin (Fig. 13d). The REE compositions of the Escabroso and Cerro de las Tórtolas Formations (lower) indicate the arc magmas migrated through a continental crust of normal thickness and that the Andean crust had not yet undergone significant tectonic shortening related to increased compression.

The combination of higher fluid-mobile/immobile incompatible TE ratios and lower fluid-immobile incompatible TE ratios obtained for the Escabroso and Cerro de las Tórtolas Formations are indicative of an increased influence of slab-derived fluids on the melt source region, and a higher degree of partial melting, in comparison to the Late Oligocene. This is supported by boron isotopic compositions and concentrations obtained from melt inclusions (Jones et al., 2014). During this time interval subduction of the JFR began along the Andean margin. The JFR has been associated with hydrated and serpentinised oceanic lithosphere (Kopp et al., 2004), hence the subduction of this hydrated ridge may account for observed increase in the influence of slab-derived fluids on the melt source region.

8.5. Mid–Late Miocene (~13–6 Ma)

During the Mid to Late Miocene the angle of the subducting Nazca plate shallowed, causing the migration of arc magmatism to the east and an increase in compression along the margin, resulting in the main phase of uplift of the Andean range (e.g., Gregory-Wodzicki, 2000; Kurtz et al., 1997). In the Pampean flat-slab segment, arc magmatism during this time interval primarily consists of the eruption of trachyandesitic to dacitic lavas of the Upper Cerro de las Tórtolas Formation in the Frontal Cordillera, and the emplacement of shallow level, sub-volcanic andesites, dacites and trachydacites in the eastern Frontal Cordillera and the Precordillera. Subsequent to this, the last significant magmatic activity in this region is represented by the eruption of small volume, dacitic to rhyolitic ignimbrites, the Vacas Heladas Ignimbrites, in the Frontal Cordillera (Fig. 13e).

Zircon inheritance and the isotopic compositions (Jones et al., 2015; Kay et al., 1991) obtained for the Vacas Heladas Ignimbrites suggests the involvement of a Grenville-aged basement, the Late Paleozoic–Early Mesozoic Andean crust, as well as Cenozoic crust in the petrogenesis of these arc magmas. The interaction of these relatively young (~6 Ma) arc magmas, erupted in the Frontal Cordillera, with a Grenville-aged basement supports a number of structural models for the southern Central Andean margin (e.g., Gans et al., 2011; Gilbert et al., 2006; Ramos et al., 2004). These models suggest the Grenville-aged basement identified in the Argentinean Precordillera (e.g., Abbruzzi et al., 1993; Kay and Orrell, 1996; Rapela et al., 2010), has under-thrust the Frontal Cordillera as a result of crustal shortening.

A principal feature of the Mid to Late Miocene arc magmatic rocks is their adakitic signatures (Fig. 12). These have been interpreted as representing the melting and equilibration of arc magmas with a high pressure mineral assemblage, which includes garnet, in the lower crust. The occurrence of adakitic signatures in the Mid to Late Miocene is consistent with the timing of significant tectonic shortening in the region and the proposed timing of the main uplift of the Andean range (e.g., Gregory-Wodzicki, 2000; Kurtz et al., 1997; Vandervoort et al., 1995). This increase in crustal thickness has been linked to the increase in compression, in part due to the shallowing of the subducting slab (e.g., Jordan et al., 1983; Kay et al., 1991). The presence of adakitic signatures in the Tertiary Intrusives, emplaced in the Argentinean Precordillera, suggests the continental crust must have thickened to >50 km at this across-arc position (western Precordillera), as well as beneath the Frontal Cordillera.

9. Conclusions

The new age data and TE and REE compositions obtained for Late Cretaceous to Late Miocene arc magmatic rocks suggest progressive, yet variable contamination of the arc magmas over time. This study clearly demonstrates the link between the changing geodynamic setting in the southern Central Andes, specifically related to changes in the angle of the subducting slab and convergence angles and rates, and the compositions of the Late Cretaceous to Late Miocene arc magmas present in the Pampean flat-slab segment.

The TE geochemistry of the Late Cretaceous to Eocene arc rocks, combined with a lack of inherited zircon, provides evidence to suggest the Late Cretaceous to Late Eocene arc magmas had little interaction with the overlying Andean crust en route to the surface. This confirms previous evidence (e.g., Jones et al., 2015; Parada, 1990; Parada et al., 1988) and is in keeping with the more extensional regime and thinner continental crust in existence during this time period. The increased enrichment of arc magmas during this time interval is proposed to be a result of the gradual enrichment of the mantle wedge due to the increased influence of subducting components and/or the influx of asthenospheric mantle.

The TE and REE compositions of the Late Oligocene (~26 Ma) to Early Miocene (~17 Ma), and Late Miocene (~6 Ma) arc magmatic rocks present in the Frontal Cordillera, combined with the presence of P–T inherited zircon cores, provides evidence for the bulk assimilation of the P–T basement by these arc magmas. The distinct TE signatures (specifically low Th, U and REE concentrations) obtained for the Tertiary Intrusives (11.7–9.4 Ma), located in the Argentinean Precordillera, combined with the presence of inherited zircon cores of Proterozoic age, suggests these arc magmas have also interacted with the Grenville-aged basement present in the Precordillera.

The progressive enrichment of arc magmas in incompatible TE between the Late Oligocene (~26 Ma) and the Late Miocene (~6 Ma) is attributed to a combination of (1) the increased influence of subducting components on the melt source region, and (2) increased contamination of the arc magmas with existing continental crust en route to the surface. Both of these processes are linked with the shallowing angle of the

subducting Nazca plate, the increased compression along the margin, and the consequent increase in crustal thickness.

Acknowledgements

We are grateful to Nic Odling and Katarzyna Sokol for assistance in XRF analysis, and to Valerie Olive for expertise and guidance in ICP-MS analysis. James Malley and Sarah Sherlock are thanked for conducting the Ar–Ar dating, and Benjamin Heit, Dante Scatolon and Eduardo Campos for help with fieldwork logistics. We would also like to express our gratitude to Mike Hall and Robert McDonald for help with sample preparation and to Nicola Cayzer for guidance in SEM imaging. Godfrey Fitton, Alan Hastie, Cees-Jan de Hoog, Simon Harley and Jon Davidson are thanked for engaging discussions relating to the content of this manuscript. This work was funded by a NERC CASE studentship (NE/G524128/1) and the Derek and Maureen Moss Scholarship. SIMS analysis at the EIMF was supported by NERC (IMF425/1010). Linda Kirstein acknowledges support from the Carnegie Trust for the Universities of Scotland. The manuscript has benefited from thorough reviews from Pat Castillo and an anonymous reviewer.

Appendix A. Supplementary data

Supplementary data to this article can be found online at <http://dx.doi.org/10.1016/j.lithos.2016.07.002>.

References

- Abbruzzi, J., Kay, S.M., Bickford, M.E., 1993. Implications for the nature of the Precordilleran basement from the geochemistry and age of Precambrian xenoliths in Miocene volcanic rocks, San Juan province. *Actas* 3, 331–339.
- Allmendinger, R., Figueroa, D., Snyder, D., Beer, J., Mpodozis, C., Isacks, B., 1990. Foreland shortening and crustal balancing in the Andes at 30°S latitude. *Tectonics* 9, 789–809.
- Astini, R.A., Benedetto, J.L., Vaccari, N.E., 1995. The early Paleozoic evolution of the Argentine Precordillera as a Laurentian rifted, drifted, and collided terrane: a geodynamic model. *Geological Society of America Bulletin* 107, 253–273.
- Beard, J.S., Ragland, P.C., Crawford, M.L., 2005. Reactive bulk assimilation: a model for crust–mantle mixing in silicic magmas. *Geology* 33, 681–684.
- Bissig, T., Lee, J.K.W., Clark, A.H., Heather, K.B., 2001. The Cenozoic History of Volcanism and Hydrothermal Alteration in the Central Andean Flat-Slab Region: new 40Ar–39Ar Constraints from the El Indio–Pascua Au (–Ag, Cu) Belt, 29°20′–30°30′ S. *International Geology Review* 43, 312–340.
- Bissig, T., Clark, A.H., Lee, J.K., von Quadt, A., 2003. Petrogenetic and metallogenic responses to Miocene slab flattening: new constraints from the El Indio–Pascua Au–Ag–Cu belt, Chile/Argentina. *Mineralium Deposita* 38, 844–862.
- Cahill, T., Isacks, B.L., 1992. Seismicity and shape of the subducted Nazca plate. *Journal of Geophysical Research: Solid Earth* (1978–2012) 97, 17503–17529.
- Cardó, R., Díaz, I.N., 1999. Hoja Geológica 3169-I, Rodeo, Provincias de San Juan. Instituto de Geología y Recursos Minerales, Servicio Geológico Minero Argentino, Buenos Aires.
- Cardó, R., Díaz, I.N., Limarino, C.O., Litvak, V.D., Poma, S., Santamaria, G., 2007. Hoja Geológica 2969-III, Malimán, provincias de San Juan y La Rioja, Boletín 320 ed. Instituto de Geología y Recursos Minerales, Servicio Geológico Minero Argentino, Buenos Aires.
- Castillo, P.R., 2012. Adakite petrogenesis. *Lithos* 134, 304–316.
- Castillo, P.R., Janney, P.E., Solidum, R.U., 1999. Petrology and geochemistry of Camiguin Island, southern Philippines: insights to the source of adakites and other lavas in a complex arc setting. *Contributions to Mineralogy and Petrology* 134, 33–51.
- Charrier, R., Pinto, L., Rodríguez, M.P., 2007. Tectonostratigraphic evolution of the Andean Orogen in Chile. In: Moreno, T., Gibbons, W. (Eds.), *The Geology of Chile*. The Geological Society, London, pp. 21–114.
- Chulick, G.S., Dettweiler, S., Mooney, W.D., 2013. Seismic structure of the crust and uppermost mantle of South America and surrounding oceanic basins. *Journal of South American Earth Sciences* 42, 260–276.
- Chung, S.-L., Liu, D., Ji, J., Chu, M.-F., Lee, H.-Y., Wen, D.-J., Lo, C.-H., Lee, T.-Y., Qian, Q., Zhang, Q., 2003. Adakites from continental collision zones: melting of thickened lower crust beneath southern Tibet. *Geology* 31, 1021–1024.
- Cribb, J.W., Barton, M., 1996. Geochemical effects of decoupled fractional crystallization and crustal assimilation. *Lithos* 37, 293–307.
- Davidson, J.P., Harmon, R.S., Wörner, G., 1991. The source of central Andean magmas; some considerations. *Geological Society of America Special Papers* 265, 233–244.
- Davidson, J., Turner, S., Handley, H., Macpherson, C., Dosseto, A., 2007. Amphibole “sponge” in arc crust? *Geology* 35, 787–790.
- Defant, M.J., Drummond, M.S., 1990. Derivation of some modern arc magmas by melting of young subducted lithosphere. *Nature* 347, 662–665.
- Drummond, M.S., Defant, M.J., 1990. A model for Trondhjemite–Tonalite–Dacite genesis and crustal growth via slab melting: archaic to modern comparisons. *Journal of Geophysical Research: Solid Earth* 95, 21503–21521.
- Emparan, C., Pineda, G., 1999. Area Condoriaco–Rivadavia, Región de Coquimbo. Servicio Nacional de Geología y Minería, Mapas Geológicos, Santiago.
- Ersay, Y., Helvacı, C., 2010. FC–AFC–FCA and mixing modeler: a Microsoft® Excel® spreadsheet program for modeling geochemical differentiation of magma by crystal fractionation, crustal assimilation and mixing. *Computers & Geosciences* 36, 383–390.
- Finney, S., 2007. The parautochthonous Gondwanan origin of the Cuyania (greater Precordillera) terrane of Argentina: a re-evaluation of evidence used to support an allochthonous Laurentian origin. *Geologica Acta: An International Earth Science Journal* 5, 127–158.
- Fitton, J.G., Godard, M., 2004. Origin and evolution of magmas on the Ontong Java Plateau. *Geological Society, London, Special Publications* 229, 151–178.
- Fitton, J.G., Saunders, A.D., Larsen, L.M., Hardarson, B.S., Norry, M.J., 1998. Volcanic rocks from the southeast Greenland margin at 63°N: composition, petrogenesis, and mantle sources. *Proceedings of the Ocean Drilling Programme Scientific Results* 152, 331–350.
- Fromm, R., Zandt, G., Beck, S.L., 2004. Crustal thickness beneath the Andes and Sierras Pampeanas at 30°S inferred from Pn apparent phase velocities. *Geophysical Research Letters* 31, L06625.
- Gans, C.R., Beck, S.L., Zandt, G., Gilbert, H., Alvarado, P., Anderson, M., Linkimer, L., 2011. Continental and oceanic crustal structure of the Pampean flat slab region, western Argentina, using receiver function analysis: new high-resolution results. *Geophysical Journal International* 186, 45–58.
- Gilbert, H., Beck, S., Zandt, G., 2006. Lithospheric and upper mantle structure of central Chile and Argentina. *Geophysical Journal International* 165, 383–398.
- Goss, A., Kay, S., Mpodozis, C., 2011. The geochemistry of a dying continental arc: the Incapillo Caldera and Dome Complex of the southernmost Central Andean Volcanic Zone (–28° S). *Contributions to Mineralogy and Petrology* 161, 101–128.
- Goss, A.R., Kay, S.M., Mpodozis, C., 2013. Andean adakite-like high-Mg andesites on the northern margin of the Chilean–Pampean flat-slab (27°–28.5° S) associated with frontal arc migration and fore-arc subduction erosion. *Journal of Petrology* 54, 2193–2234.
- Gregory-Wodzicki, K.M., 2000. Uplift history of the Central and Northern Andes: a review. *Geological Society of America Bulletin* 112, 1091–1105.
- Gutscher, M.-A., Maury, R., Eissen, J.-P., Bourdon, E., 2000a. Can slab melting be caused by flat subduction? *Geology* 28, 535–538.
- Gutscher, M.A., Spakman, W., Bijwaard, H., Engdahl, E.R., 2000b. Geodynamics of flat subduction: seismicity and tomographic constraints from the Andean margin. *Tectonics* 19, 814–833.
- Hildreth, W., Moorbath, S., 1988. Crustal contributions to arc magmatism in the Andes of Central Chile. *Contributions to Mineralogy and Petrology* 98, 455–489.
- Irvine, T., Baragar, W., 1971. A guide to the chemical classification of the common volcanic rocks. *Canadian Journal of Earth Sciences* 8, 523–548.
- Jacques, G., Hoernle, K., Gill, J., Hauff, F., Wehrmann, H., Garbe-Schönberg, D., van den Bogaard, P., Bindeman, I., Lara, L., 2013. Across-arc geochemical variations in the Southern Volcanic Zone, Chile (34.5°–38.0° S): constraints on mantle wedge and slab input compositions. *Geochimica et Cosmochimica Acta* 123, 218–243.
- James, D.E., 1982. A combined O, Sr, Nd and Pb isotopic and trace element study of crustal contamination in central Andean lavas. I. Local geochemical variations. *Earth and Planetary Science Letters* 57, 47–62.
- Jarvis, A., Reuter, H.L., Nelson, A., Guevara, E., 2008. Hole-filled SRTM for the Globe Version 4, Available from the CGIAR-CSI SRTM 90m Database.
- JICA-MMAR, 1999. In: SEGEMAR (Ed.), *Informe de la exploración de mineral en la región Cordillera Oriental Andina, República Argentina*, p. 164 Buenos Aires.
- Jones, R.E., De Hoog, J.C.M., Kirstein, L.A., Kasemann, S.A., Hinton, R., Elliott, T., Litvak, V.D., 2014. Temporal variations in the influence of the subducting slab on Central Andean arc magmas: evidence from boron isotope systematics. *Earth and Planetary Science Letters* 408, 390–401.
- Jones, R.E., Kirstein, L.A., Kasemann, S.A., Dhuime, B., Elliott, T., Litvak, V.D., Alonso, R., Hinton, R., 2015. Geodynamic controls on the contamination of Cenozoic arc magmas in the southern Central Andes: insights from the O and Hf isotopic composition of zircon. *Geochimica et Cosmochimica Acta* 164, 386–402.
- Jordan, T.E., Isacks, B.L., Allmendinger, R.W., Brewer, J.A., Ramos, V.A., Ando, C.J., 1983. Andean tectonics related to geometry of subducted Nazca plate. *Geological Society of America Bulletin* 94, 341–361.
- Kay, R.W., 1978. Aleutian magnesian andesites: melts from subducted Pacific ocean crust. *Journal of Volcanology and Geothermal Research* 4, 117–132.
- Kay, S.M., Abbruzzi, J.M., 1996. Magmatic evidence for Neogene lithospheric evolution of the central Andean “flat slab” between 30°S and 32°S. *Tectonophysics* 259, 15–28.
- Kay, S., Gordillo, C., 1994. Pocho volcanic rocks and the melting of depleted continental lithosphere above a shallowly dipping subduction zone in the central Andes. *Contributions to Mineralogy and Petrology* 117, 25–44.
- Kay, S.M., Mpodozis, C., 2002. Magmatism as a probe to the Neogene shallowing of the Nazca plate beneath the modern Chilean flat slab. *Journal of South American Earth Sciences* 15, 39–57.
- Kay, S.M., Orrell, S., 1996. Zircon and whole rock Nd–Pb isotopic evidence for a Grenville age and a Laurentian origin for the Basement of the Precordillera in Argentina. *Journal of Geology* 104, 637.
- Kay, S.M., Maksav, V., Moscoso, R., Mpodozis, C., Nasi, C., 1987. Probing the evolving Andean lithosphere: Mid–Late Tertiary magmatism in Chile (29°–30°30′S) over the modern zone of subhorizontal subduction. *Journal of Geophysical Research* 92, 6173–6189.
- Kay, S.M., Ramos, V.A., Mpodozis, C., Sruoga, P., 1989. Late Paleozoic to Jurassic silicic magmatism at the Gondwana margin: analogy to the Middle Proterozoic in North America? *Geology* 17, 324–328.

- Kay, S.M., Mpodozis, C., Ramos, V.A., Munizaga, F., 1991. Magma source variations for mid-late Tertiary magmatic rocks associated with a shallowing subduction zone and the thickening crust in the central Andes (28–33°S). *Spec. Pap. Geological Society of America Bulletin* 265, 113–137.
- Kay, S.M., Orrell, S., Abbruzzi, J.M., 1996. Zircon and whole rock Nd–Pb isotopic evidence for a Grenville age and a Laurentian origin for the basement of the Precordillera in Argentina. *The Journal of Geology* 104, 637–648.
- Kay, S.M., Godoy, E., Kurtz, A., 2005. Episodic arc migration, crustal thickening, subduction erosion, and magmatism in the south-central Andes. *Geological Society of America Bulletin* 117, 67–88.
- Keller, M., 1999. Argentine precordillera: sedimentary and plate tectonic history of a Laurentian crustal fragment in South America. *Geological Society of America Special Papers* 341, 1–131.
- Kelly, N., Hinton, R., Harley, S., Appleby, S., 2008. New SIMS U–Pb zircon ages from the Langavat Belt, South Harris, NW Scotland: implications for the Lewisian terrane model. *Journal of the Geological Society* 165, 967–981.
- Kilian, R., Behrmann, J.H., 2003. Geochemical constraints on the sources of Southern Chile Trench sediments and their recycling in arc magmas of the Southern Andes. *Journal of the Geological Society* 160, 57–70.
- Kirby, S., Engdahl, R.E., Denlinger, R., 1996. Intermediate-depth intraslab earthquakes and arc volcanism as physical expressions of crustal and uppermost mantle metamorphism in subducting slabs. Subduction top to bottom, pp. 195–214.
- Kopp, H., Flueh, E.R., Papenberg, C., Klaeschen, D., 2004. Seismic investigations of the O'Higgins Seamount Group and Juan Fernández Ridge: aseismic ridge emplacement and lithosphere hydration. *Tectonics* 23.
- Kurtz, A.C., Kay, S.M., Charrier, R., Farrar, E., 1997. Geochronology of Miocene plutons and exhumation history of the El Teniente region, Central Chile (34–35° S). *Andean Geology* 24, 75–90.
- Le Maitre, R.W., Bateman, P., Dudek, A., Keller, J., Lameyre, J., Le Bas, M., Sabine, P., Schmid, R., Sorensen, H., Streckeisen, A., 1989. A Classification of Igneous Rocks and Glossary of Terms: Recommendations of the International Union of Geological Sciences Subcommittee on the Systematics of Igneous Rocks. Blackwell Oxford.
- Leveratto, M., 1976. Edad de intrusivos cenozoicos en la Precordillera de San Juan y su implicancia estratigráfica. *Revista de la Asociación Geológica Argentina* 31, 53–58.
- Limarino, C.O., Gutiérrez, P.R., Malizia, D., Barreda, V., Page, S., Ostera, H., Linares, E., 1999. Edad de las secuencias paleógenas y neógenas de las cordilleras de La Brea y Zancarrón, Valle del Cura, San Juan. *Revista de la Asociación Geológica Argentina* 54, 177–181.
- Litvak, V.D., Page, S., 2002. Nueva evidencia cronológica en el Valle del Cura, provincia de San Juan, Argentina. *Revista de la Asociación Geológica Argentina* 57, 483–486.
- Litvak, V.D., Poma, S., 2005. Estratigrafía y facies volcánicas y volcanoclásticas de la Formación Valle del Cura: magmatismo paleógeno en la Cordillera Frontal de San Juan. *Revista de la Asociación Geológica Argentina* 60, 402–416.
- Litvak, V.D., Poma, S., 2010. Geochemistry of mafic Paleocene volcanic rocks in the Valle del Cura region: implications for the petrogenesis of primary mantle-derived melts over the Pampean flat-slab. *Journal of South American Earth Sciences* 29, 705–716.
- Litvak, V.D., Kay, S.M., Mpodozis, M., 2005. New K/Ar ages on Tertiary Volcanic Rocks in the Valle del Cura, Pampean flat slab segment, Argentina. *Actas XVI Congreso Geológico Argentino* 2, 159–164.
- Litvak, V.D., Poma, S., Kay, S.M., 2007. Paleogene and Neogene magmatism in the Valle del Cura region: new perspective on the evolution of the Pampean flat slab, San Juan province, Argentina. *Journal of South American Earth Sciences* 24, 117–137.
- Llambías, E.J., Sato, A.M., 1990. El Batolito de Colangüil (29–31° S) cordillera frontal de Argentina: estructura y marco tectónico. *Andean Geology* 17, 89–108.
- Llambías, E.J., Sato, A.M., 1995. El batolito de Colangüil: transición entre orogénesis y anorogénesis. *Revista de la Asociación Geológica Argentina* 50, 111–131.
- Llambías, E.J., Shaw, S., Sato, A.M., 1990. Lower Miocene plutons in the Eastern Cordillera frontal of San Juan (29° 75' S, 69° 30' W). 11° Congreso Geológico Argentino, San Juan, pp. 83–86.
- Lonsdale, P., 2005. Creation of the Cocos and Nazca plates by fission of the Farallon plate. *Tectonophysics* 404, 237–264.
- Lucassen, F., Harmon, R., Franz, G., Romer, R.L., Becchio, R., Siebel, W., 2002. Lead evolution of the Pre-Mesozoic crust in the Central Andes (18–27°): progressive homogenisation of Pb. *Chemical Geology* 186, 183–197.
- Lucassen, F., Wiedicke, M., Franz, G., 2010. Complete recycling of a magmatic arc: evidence from chemical and isotopic composition of Quaternary trench sediments in Chile (36°–40°S). *International Journal of Earth Sciences* 99, 687–701.
- Ludwig, K.R., 2008. User's Manual for Isoplot 3.7 – A Geochronological Toolkit for Microsoft Excel. Berkeley Geochronology Center Special Publication 4.
- Macpherson, C.G., Dreher, S.T., Thirlwall, M.F., 2006. Adakites without slab melting: high pressure differentiation of island arc magma, Mindanao, the Philippines. *Earth and Planetary Science Letters* 243, 581–593.
- Maksaev, V., Moscoso, R., Mpodozis, C., Nasi, C., 1984. Las unidades volcánicas y plutónicas del Cenozoico superior en la Alta Cordillera del Norte Chico (29°–31° S): Geología, Alteración hidrotermal y Mineralización. *Revista Geológica de Chile* 11, 12–51.
- Martin, M.W., Clavero, R., J., Mpodozis, M., C., Cuitiño, L., 1995. Estudio Geológico de la Franja El Indio, Cordillera de Coquimbo. Servicio Nacional de Geología y Minería, Santiago.
- Martin, M.W., Clavero, R., J., Mpodozis, M., C., 1997. Eocene to Late Miocene magmatic development of El Indio Belt, 30° S, North-central Chile, Congreso Geológico Chileno, 8 Actas 1, Antofagasta, pp. 149–153.
- Martin, M.W., Clavero, R., J., Mpodozis, M., C., 1999. Late Paleozoic to Early Jurassic tectonic development of the high Andean Principal Cordillera, El Indio Region, Chile (29–30°S). *Journal of South American Earth Sciences* 12, 33–49.
- McGlashan, N., Brown, L., Kay, S., 2008. Crustal thickness in the central Andes from teleseismically recorded depth phase precursors. *Geophysical Journal International* 175, 1013–1022.
- Mpodozis, C., Cornejo, P.P., 1988. Hoja Pisco Elqui, Region de Coquimbo. In: Mpodozis, C., Davidson, J., Rivano, S. (Eds.), *Carta Geologica de Chile*. Servicio Nacional de Geología y Minería (SERNAGEOMIN), Santiago.
- Mpodozis, C., Kay, S.M., 1990. Provincias magmáticas ácidas y evolución tectónica de Gondwana: Andes chilenos (28–31° S). *Andean Geology* 17, 153–180.
- Mpodozis, C., Kay, S.M., 1992. Late Paleozoic to Triassic evolution of the Gondwana margin: evidence from Chilean Frontal Cordilleran batholiths (28° S to 31° S). *Geological Society of America Bulletin* 104, 999–1014.
- Nasi, C., Mpodozis, M., C., Cornejo, P., Moscoso, R., Maksaev, V., 1985. El Batolito Elqui-Limarí (Paleozoico Superior Triásico): características petrográficas, geoquímicas y significado tectónico. *Revista Geológica de Chile* 25, 26.
- Nasi, C., Moscoso, R., Maksaev, V., 1990. Hoja Guanta, Regiones de Atacama y Coquimbo. In: Mpodozis, C., Davidson, J., Rivano, S. (Eds.), *Carta Geologica de Chile*. Servicio Nacional de Geología y Minería (SERNAGEOMIN), Santiago.
- Nur, A., Ben-Avraham, Z., 1981. Volcanic gaps and the consumption of aseismic ridges in South America. *Geological Society of America Memoirs* 154, 729–740.
- O'Driscoll, L.J., Richards, M.A., Humphreys, E.D., 2012. Nazca–South America interactions and the late Eocene–late Oligocene flat-slab episode in the central Andes. *Tectonics* 31.
- Parada, M.A., 1990. Granitoid plutonism in central Chile and its geodynamic implications; a review. In: Kay, S.M., Rapela, C.W. (Eds.), *Plutonism from Antarctica to Alaska*. The Geological Society of America, Boulder, Colorado.
- Parada, M.A., Rivano, S., Sepulveda, P., Herve, M., Herve, F., Puig, A., Munizaga, F., Brook, M., Pankhurst, R., Snelling, N., 1988. Mesozoic and Cenozoic plutonic development in the Andes of central Chile (30°30'–32°30'S). *Journal of South American Earth Sciences* 1, 249–260.
- Parada, M.A., López-Escobar, L., Oliveros, V., Fuentes, F., Morata, D., Calderón, M., Aguirre, L., Féraud, G., Espinoza, F., Moreno, H., Figueroa, O., Bravo, J.M., Vásquez, R.T., Stern, C.R., 2007. Andean magmatism. In: Moreno, T., Gibbons, W. (Eds.), *The Geology of Chile*. The Geological Society, London, pp. 115–146.
- Pardo Casas, F., Molnar, P., 1987. Relative motion of the Nazca (Farallón) and South America plates since Late Cretaceous time. *Tectonics* 6, 233–248.
- Pearce, J.A., 2008. Geochemical fingerprinting of oceanic basalts with applications to ophiolite classification and the search for Archean oceanic crust. *Lithos* 100, 14–48.
- Pilger, R.H., 1981. Plate reconstructions, aseismic ridges, and low angle subduction beneath the Andes. *Geological Society of America Bulletin* 92, 448–456.
- Pilger, R.H., 1984. Cenozoic plate kinematics, subduction and magmatism: South American Andes. *Journal of Geological Society London* 141, 793–802.
- Pineda, G., Calderón, M., 2008. Geología del área Monte Patria-El Maqui, Región de Coquimbo, Carta Geológica de Chile, Serie Geología Básica. Servicio Nacional de Geología y Minería, Santiago.
- Pineda, G., Emparan, C., 2006. Geología del área Vicuña-Pichasca, Región de Coquimbo, Carta Geológica de Chile, Serie Geología Básica. Servicio Nacional de Geología y Minería, Santiago.
- Plank, T., Langmuir, C.H., 1998. The chemical composition of subducting sediment and its consequences for the crust and mantle. *Chemical Geology* 145, 325–394.
- Poma, S., Limarino, C., Litvak, V., 2005. Formación Las Trancas: expresión del arco magmático terciario en el faldeo occidental de la Precordillera de San Juan. *Actas, Congreso Geológico Argentino*, 16th, La Plata. Asociación Geológica Argentina, Buenos Aires, pp. 331–334.
- Ramos, V.A., Kay, S.M., Page, R., Munizaga, F., 1989. La Ignimbrita Vacas Heladas y el cese del volcanismo en el valle del Cura, provincia de San Juan. *Revista de la Asociación Geológica Argentina* 44, 336–352.
- Ramos, V.A., Cristallini, E., Pérez, D.J., 2002. The Pampean flat-slab of the Central Andes. *Journal of South American Earth Sciences* 15, 59–78.
- Ramos, V.A., Zapata, T., Cristallini, E., Introcaso, A., 2004. The Andean thrust system—latitudinal variations in structural styles and orogenic shortening. *Thrust Tectonics and Hydrocarbon Systems* 82, 30–50.
- Rapela, C., Pankhurst, R., Casquet, C., Baldo, E., Saavedra, J., Galindo, C., 1998. Early evolution of the Proto-Andean margin of South America. *Geology* 26, 707–710.
- Rapela, C.W., Pankhurst, R.J., Casquet, C., Baldo, E., Galindo, C., Fanning, C.M., Dahlquist, J.M., 2010. The Western Sierras Pampeanas: Protracted Grenville-age history (1330–1030 Ma) of intra-oceanic arcs, subduction-accretion at continental-edge and AMCG intraplate magmatism. *Journal of South American Earth Sciences* 29, 105–127.
- Reich, M., Parada, M.A., Palacios, C., Dietrich, A., Schultz, F., Lehmann, B., 2003. Adakite-like signature of Late Miocene intrusions at the Los Pelambres giant porphyry copper deposit in the Andes of central Chile: metallogenic implications. *Mineralium Deposita* 38, 876–885.
- Richards, J.P., Kerrich, R., 2007. Special paper: adakite-like rocks: their diverse origins and questionable role in metallogenesis. *Economic Geology* 102, 537–576.
- Rodríguez, C., Sellés, D., Dungan, M., Langmuir, C., Leeman, W., 2007. Adakitic dacites formed by intracrustal crystal fractionation of water-rich parent magmas at Nevado de Longaví Volcano (36°2'S; Andean Southern Volcanic Zone, Central Chile). *Journal of Petrology* 48, 2033–2061.
- Rooney, T., Franceschi, P., Hall, C., 2011. Water-saturated magmas in the Panama Canal region: a precursor to adakite-like magma generation? *Contributions to Mineralogy and Petrology* 161, 373–388.
- Sato, A.M., Llambías, E.J., Basei, M.A.S., Castro, C.E., 2015. Three stages in the Late Paleozoic to Triassic magmatism of southwestern Gondwana, and the relationships with the volcanogenic events in coeval basins. *Journal of South American Earth Sciences* 63, 48–69.
- Sigmarsson, O., Condomines, M., Morris, J.D., Harmon, R.S., 1990. Uranium and 10Be enrichments by fluids in Andean arc magmas. *Nature* 346, 163–165.
- Silver, P.G., Russo, R.M., Lithgow-Bertelloni, C., 1998. Coupling of South American and African plate motion and plate deformation. *Science* 279, 60–63.

- Somoza, R., 1998. Updated azca (Farallon)–South America relative motions during the last 40 My: implications for mountain building in the central Andean region. *Journal of South American Earth Sciences* 11, 211–215.
- Somoza, R., Ghidella, M.E., 2012. Late Cretaceous to recent plate motions in western South America revisited. *Earth and Planetary Science Letters* 331–332, 152–163.
- Stern, C.R., 1991. Role of subduction erosion in the generation of Andean magmas. *Geology* 19, 78–81.
- Stern, C.R., 2004. Active Andean volcanism: its geologic and tectonic setting. *Revista Geológica de Chile* 31, 161–206.
- Stern, C.R., Kilian, R., 1996. Role of the subducted slab, mantle wedge and continental crust in the generation of adakites from the Andean Austral Volcanic Zone. *Contributions to Mineralogy and Petrology* 123, 263–281.
- Stern, C.R., Skewes, M.A., 1995. Miocene to present magmatic evolution at the northern end of the Andean Southern Volcanic Zone, Central Chile. *Andean Geology* 22, 261–272.
- Sun, S.S., McDonough, W.F., 1989. Chemical and isotopic systematics of oceanic basalts: implications for mantle compositions and processes. Geological Society, London, Special Publications 42, 313–345.
- Syracuse, E.M., van Keken, P.E., Abers, G.A., 2010. The global range of subduction zone thermal models. *Physics of the Earth and Planetary Interiors* 183, 73–90.
- Taylor, S.R., McLennan, S.M., 1995. The geochemical evolution of the continental crust. *Reviews of Geophysics* 33, 241–265.
- Thomas, W.A., Astini, R.A., 2003. Ordovician accretion of the Argentine Precordillera terrane to Gondwana: a review. *Journal of South American Earth Sciences* 16, 67–79.
- Thomas, W.A., Astini, R.A., Mueller, P.A., Gehrels, G.E., Wooden, J.L., 2004. Transfer of the Argentine Precordillera terrane from Laurentia: constraints from detrital-zircon geochronology. *Geology* 32, 965–968.
- Vandervoort, D.S., Jordan, T.E., Zeitler, P.K., Alonso, R.N., 1995. Chronology of internal drainage development and uplift, southern Puna plateau, Argentine central Andes. *Geology* 23, 145–148.
- Völker, D., Geersen, J., Contreras-Reyes, E., Reichert, C., 2013. Sedimentary fill of the Chile Trench (32–46°S): volumetric distribution and causal factors. *Journal of the Geological Society* 170, 723–736.
- von Huene, R., Corvalán, J., Flueh, E., Hinz, K., Korstgard, J., Ranero, C., Weinrebe, W., 1997. Tectonic control of the subducting Juan Fernández Ridge on the Andean margin near Valparaíso, Chile. *Tectonics* 16, 474–488.
- Wetten, A.F., 2005. Andesita Cerro Bola: Nueva unidad vinculada al magmatismo mioceno de la Cordillera de Olivares, San Juan, Argentina (30° 35' S; 69° 30' O). *Revista de la Asociación Geológica Argentina* 60, 003–008.
- Wilson, B.M., 1989. *Igneous Petrogenesis A Global Tectonic Approach*. Springer.
- Winocur, D., Litvak, V., Ramos, V., 2015. Magmatic and tectonic evolution of the Oligocene Valle del Cura basin, main Andes of Argentina and Chile: evidence for generalized extension. Geological Society, London, Special Publications 399, 109–130.
- Wörner, G., Moorbath, S., Harmon, R.S., 1992. Andean Cenozoic volcanic centers reflect basement isotopic domains. *Geology* 20, 1103–1106.
- Yañez, G.A., Ranero, C.R., von Huene, R., Díaz, J., 2001. Magnetic anomaly interpretation across the southern central Andes (32°–34°S): the role of the Juan Fernández Ridge in the late Tertiary evolution of the margin. *Journal of Geophysical Research* 106, 6325–6345.
- Yañez, G.A., Cembrano, J., Pardo, M., Ranero, C.R., Selles, D., 2002. The Challenger–Juan Fernández–Maipo major tectonic transition of the Nazca–Andean subduction system at 33–34°S: geodynamic evidence and implications. *Journal of South American Earth Sciences* 15, 28–38.